Sustainable Energy & Fuels

ROYAL SOCIETY OF CHEMISTRY

REVIEW

View Article Online
View Journal | View Issue

Cite this: *Sustainable Energy Fuels*, 2025, 9, 2261

Advancements in CO_2 conversion technologies: a comprehensive review on catalyst design strategies for high-performance CO_2 methanation

Amisha Beniwal,[a] Ashima Bagaria,[b] Tsan-Yao Chen *[a] and Dinesh Bhalothia*[ac]

The increasing levels of atmospheric carbon dioxide (CO_2) have raised significant environmental concerns, driving the development of innovative solutions to mitigate its impact. CO_2 methanation, a catalytic process that converts CO_2 into methane (CH_4), has emerged as a promising technology for carbon recycling and renewable energy storage. This review critically examines the advancements in catalyst design strategies aimed at enhancing the efficiency and stability of CO_2 methanation. The focus spans monometallic and multimetallic catalysts, elucidating their roles in optimizing catalytic performance. Additionally, the importance of support materials in stabilizing active sites and facilitating electron transfer is discussed in detail. Key mechanisms, such as the creation of oxygen vacancies, surface and interface engineering, and defect engineering, are highlighted for their contributions to improving reaction kinetics and resistance to deactivation. The interplay between these strategies and their impact on the catalytic properties is analyzed, providing insights into their underlying principles. The review further addresses current challenges, including scalability, energy efficiency, and environmental considerations, while exploring emerging trends such as the integration of renewable energy in methanation processes. By synthesizing recent developments and identifying future research directions, this study aims to serve as a comprehensive resource for researchers and industry stakeholders seeking to advance the field of CO_2 conversion and contribute to global efforts toward carbon neutrality.

Received 4th February 2025
Accepted 10th March 2025

DOI: 10.1039/d5se00167f

rsc.li/sustainable-energy

1. Introduction

The dual crisis of climate change and energy security have brought carbon dioxide (CO_2) to the forefront of scientific and industrial discourse. Anthropogenic CO_2 emissions, primarily driven by fossil fuel combustion, industrial processes, and

[a]*Department of Engineering and System Science, National Tsing Hua University, Hsinchu 30013, Taiwan. E-mail: chencaeser@gmail.com; dinesh.bhalothia@jaipur.manipal.edu; Fax: +886-3-5720724*

[b]*Department of Physics, Manipal University Jaipur, Rajasthan 303007, India*

[c]*Department of Electronics and Communication Engineering, Manipal University Jaipur, Rajasthan 303007, India*

Amisha Beniwal

Amisha Beniwal is pursuing a PhD in the Department of Engineering and System Science at National Ting Hua University, Taiwan. Her research areas mainly focus on the development of oxygen vacancies enriched transition metal-based heterogeneous nanomaterials for CO_2 methanation.

Ashima Bagaria

Dr Ashima is a Professor in the Department of Physics and Associate Dean of SPBS at Manipal University Jaipur. She obtained her PhD from the Department of Physics, Indian Institute of Science, Bangalore, Karnataka. She has more than 17 years of research and teaching experience. Her research experience includes her post-doctoral experience at the Yale School of Medicine, Yale University, Connecticut USA, an Ivy League University, Brookhaven National Laboratory, New York, USA and Institute Pasteur, Paris, France.

deforestation, have escalated atmospheric concentrations of this greenhouse gas to unprecedented levels.[1] This surge in CO_2 is a significant driver of global warming, which manifests in rising temperatures, melting polar ice caps, and more frequent extreme weather events. Concurrently, the depletion of non-renewable energy resources necessitates a transition to sustainable energy systems, wherein CO_2 can serve as a valuable feedstock for chemical and fuel production.[2] Recycling atmospheric CO_2 into valuable fuels or chemicals offers a promising strategy for addressing climate change and resource sustainability. Transforming CO_2 into fuels not only integrates seamlessly with existing fuel infrastructure but also contributes to reducing global atmospheric CO_2 levels. Among various processes for CO_2 conversion, heterogeneous catalytic conversion of CO_2 into methane (CH_4), commonly referred as CO_2 methanation, stands out as a promising method.[3] This process, also known as the "Sabatier reaction," involves the reaction between CO_2 and hydrogen (H_2) to yield CH_4 and water (H_2O). Given the challenges associated with hydrogen (H_2) storage, transportation, and large-scale utilization, alongside the established industrial applications of CH_4, the combination of CO_2 with H_2 to produce CH_4 through the CO_2 methanation reaction presents a practical and effective solution (Fig. 1).[4] The significance of CO_2 methanation lies in its dual role of reducing CO_2 emissions and producing a renewable energy resource. It offers a sustainable approach to treating CO_2 not merely as a waste product but as a valuable resource. Additionally, CH_4, as a clean-burning fuel, bridges the gap between conventional fossil fuels and renewable energy, thereby facilitating the transition towards a more sustainable energy ecosystem. More importantly, this process utilizes waste industrial heat to simultaneously reduce carbon and heat emissions while avoiding significant infrastructure costs. CO_2 methanation is an exothermic reaction ($CO_2 + 4H_2 \rightarrow CH_4 + 2H_2O$, $\Delta H°298\ K = -164\ kJ\ mol^{-1}$), but its efficiency is thermodynamically constrained at high temperatures.[5] Despite its advantages, the CO_2 methanation process faces several challenges.[6] Being an exothermic reaction, it is more effective at lower temperatures for achieving high CH_4 yields.[6] However, the stability of the linear CO_2 molecule necessitates highly active catalysts to enable its activation at low temperatures.[7] Furthermore, the competitive reverse water–gas shift (RWGS) reaction, which produces carbon monoxide (CO) and water, poses a significant challenge to achieving optimal CH_4 production under these conditions.[8] Catalysts are central to the success of heterogeneous CO_2 methanation, as they facilitate the activation and transformation of CO_2 and H_2. Typically, these catalysts consist of metal nanoparticles supported on high-surface-area materials such as oxides, carbides, or nitrides.[9] The choice of catalyst composition, structural properties, and morphology plays a pivotal role in determining the reaction kinetics, selectivity, and overall efficiency of the methanation process.

Tsan-Yao Chen

Professor Chen Tsan-Yao is the Deputy Head of the Department of Engineering and System Sciences at National Tsing Hua University. With more than 13 years of experience in Materials Characterization and 6 years of experience in Electronic Device (MEMS and IC) failure analysis of multiple executives by Synchrotron Light Source Techniques (at NSRRC, Taiwan). He conducts fundamental materials development in green energy applications including solar cells, fuel cells, and CO_2 conversion, water sensing with worldwide collaboration at the national rank research teams in Russia, USA, Italy, Japan (SPring-8), and the UK. Hosting research projects from academic and industrial funds on physical chemistry research and environment sensing technologies. He heads a group of nanocrystal design and fabrication for energy conversion applications. The main work in his group is atomic cluster decoration techniques for modifying the redox performance of catalysts by incorporating interdisciplinary, and multi-scales mechanisms in heterogeneous catalysis. The work is strongly motivated by emerging real-life problems and their challenges in green energy. His group correctly works with 3 domestic groups, 1 TW company, and 2 international groups (UK@UoL and SP-8@Japan).

Dinesh Bhalothia

Dr Dinesh Bhalothia earned his PhD degree from the Institute of Electronics Engineering at National Ting Hua University, Taiwan in 2019. Currently, he is working as an Associate Professor at the Department of Electronic and Communication Engineering at Manipal University Jaipur. His area of research mainly focuses on the development of heterogeneous nanocatalysts and in situ investigation of their physical and chemical properties via synchrotron X-ray (XAS, PFY-XAS, XRD and APXPS) characterizations for green energy applications (fuel cells, CO_2 reduction and hydrogen production).

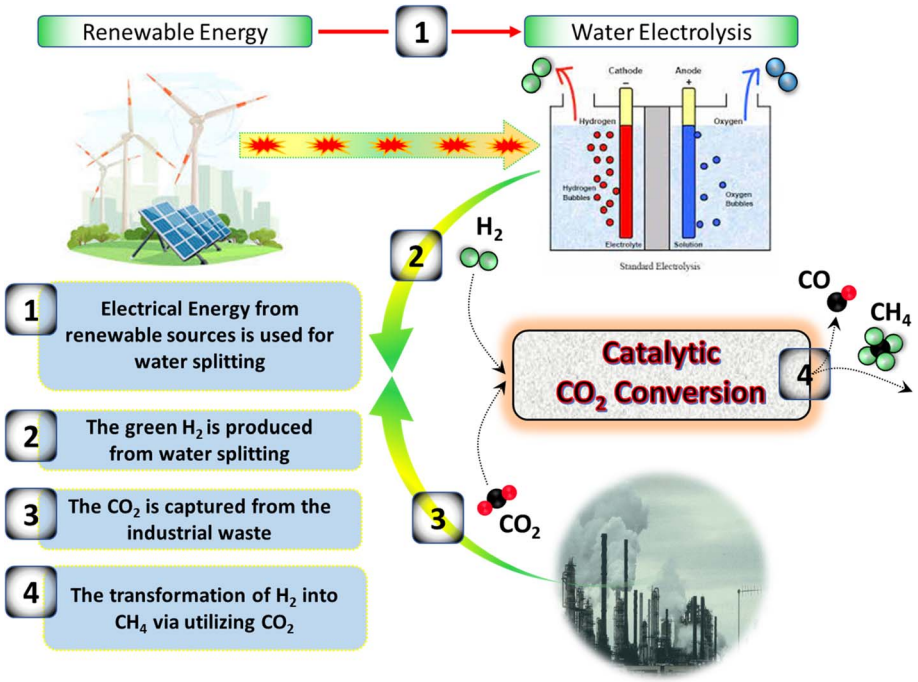

Fig. 1 Schematic representations of the closed carbon loop.

As shown in Fig. 2, heterogeneous CO_2 methanation typically proceeds through three key stages: (i) adsorption of reactants on the catalyst surface, (ii) formation of intermediate species, and (iii) desorption of the final products.[10] According to Sabatier's principle, the adsorption energy of intermediates on the catalyst surface must be finely balanced to ensure optimal reaction kinetics.[11] If the adsorption energy is too low, the bond-breaking steps of the reactants may be inefficient. Conversely, if the adsorption energy is too high, it can hinder the desorption of the final products, affecting the overall efficiency of the process. In recent years, substantial research efforts have focused on overcoming these challenges and advancing the field of CO_2 methanation. Strategies such as designing and synthesizing advanced catalysts, optimizing reaction conditions, and enhancing the mechanistic understanding of the process have been explored to improve catalyst performance.[12,13] These efforts aim to increase reaction efficiency, reduce operational costs, and ensure the scalability of CO_2 methanation for industrial applications. This review provides a comprehensive analysis of recent advancements in catalyst design strategies for high-performance CO_2 methanation. Key topics include the development of monometallic and multimetallic catalysts, the role of support materials, the influence of oxygen vacancies, and the application of surface, interface and defect engineering techniques. By synthesizing current knowledge and identifying research gaps, this review aims to guide future developments in the field, contributing to the broader goals of sustainable energy and environmental remediation. These discussions encompass innovative approaches in catalyst design, enhanced understanding of reaction mechanisms, and the implementation of

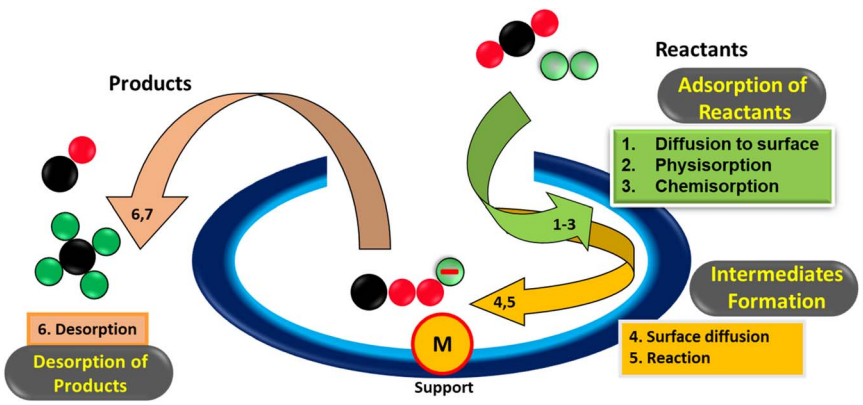

Fig. 2 The reaction pathways for heterogeneous catalytic CO_2 methanation.

optimized process parameters to achieve higher CH_4 yields and improved catalyst stability.

2. Reaction pathways for CO_2 methanation

Understanding the detailed mechanisms and identifying key intermediates in CO_2 methanation reactions is crucial for the development of high-performance catalysts. Extensive research has been conducted to elucidate the underlying mechanisms, employing both experimental approaches and theoretical modeling.[14,15] While the specific intermediates and pathways leading to CH_4 formation remain subjects of scientific debate, two primary pathways have emerged as widely accepted: the associative and dissociative mechanisms, illustrated in Fig. 3. In the associative mechanism, adsorbed CO_2 undergo a reaction with adsorbed hydrogen atoms (H^*), leading to the formation of intermediates such as formate (*HCOO) or carboxylate (*COOH). These intermediates are then progressively hydrogenated, resulting in CH_4 formation. This pathway can be further categorized into the formate route and the reverse water–gas shift (RWGS) route, depending on the specific intermediate involved in the reaction.[16,17] Conversely, the dissociative pathway, often referred to as the CO pathway, involves the initial dissociation of chemisorbed CO_2 species into *CO and *O.[18] The subsequent reaction steps then facilitate the hydrogenation of these species, ultimately yielding methane. These pathways offer insights into the reaction dynamics, highlighting the complexity of the processes involved. Further elaboration on the associative and dissociative pathways is provided in subsequent sections, shedding light on their unique characteristics and implications for catalyst design.

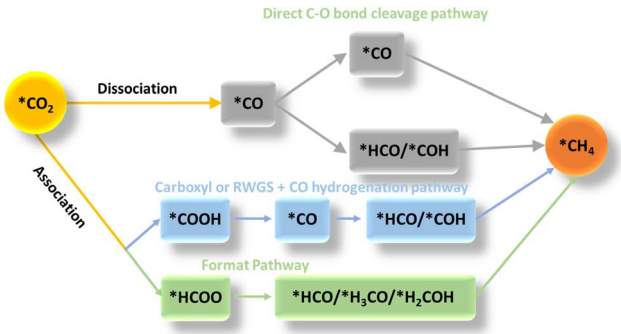

Fig. 3 Schematic representation of possible reaction pathways of CO_2 methanation.

2.1. Associative pathway

The associative pathways of CO_2 methanation involve the stepwise addition of hydrogen (H*) atoms to adsorbed CO_2 molecules (*CO_2), culminating in the production of methane (CH_4) and potential by-products. These pathways are distinguished by their reliance on intermediate species formed during the reaction process, with subsequent hydrogenation steps leading to the final methane product. Unlike dissociative

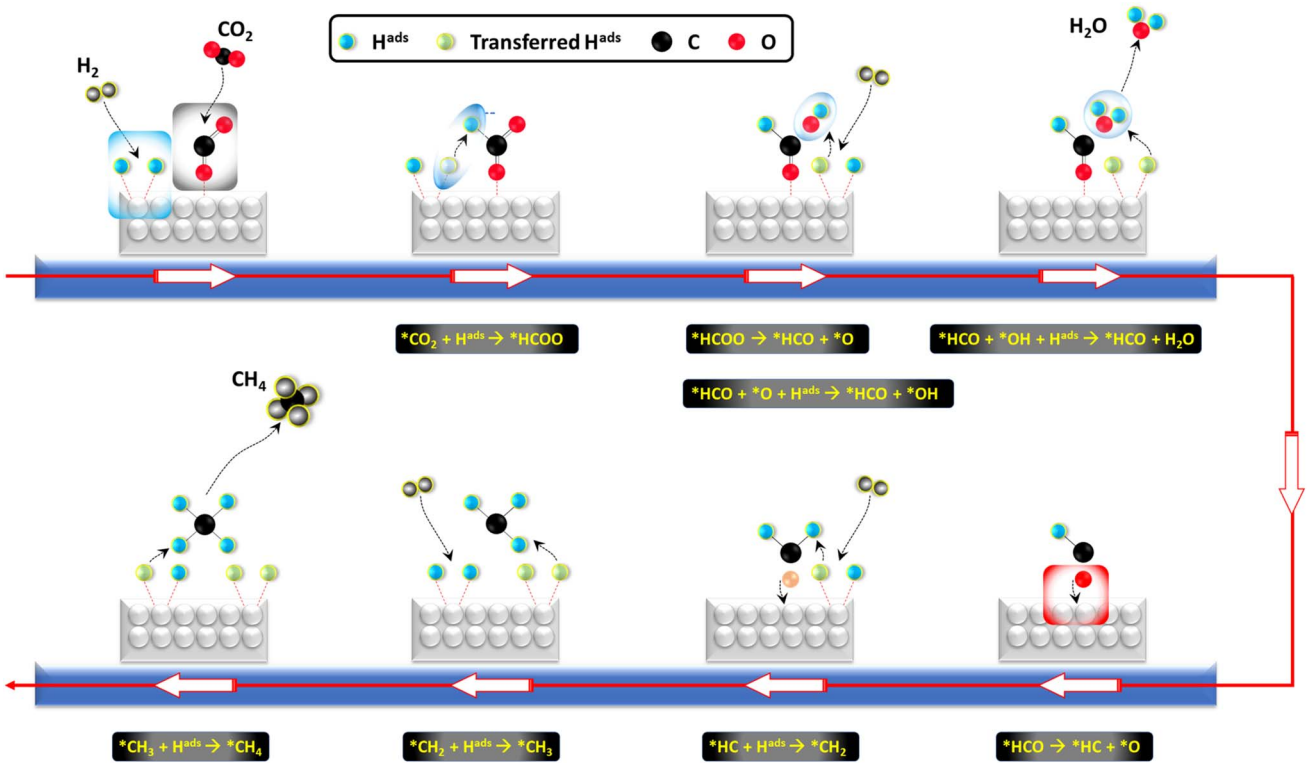

Fig. 4 The formate reaction pathway of CO_2 methanation.

pathways, the associative mechanism does not require the prior breakdown of CO_2 into carbon monoxide (CO) and oxygen (O) species. One of the most widely recognized associative mechanisms is the formate pathway, also referred to as CO_2 associative methanation.[16] As illustrated in Fig. 4, this pathway begins with the chemisorption of CO_2 molecules onto the catalyst's surface, typically through interaction with the oxygen center. The adsorbed CO_2 is then converted into bidentate formates (HCOO*), which act as key intermediate species. These formates undergo a series of hydrogenation reactions, resulting in the formation of formic acid (HCOOH). In the final stages, formic acid is further hydrogenated to produce methane (CH_4). The formate pathway highlights the direct incorporation of CO_2 into reaction intermediates, streamlining its subsequent transformation into methane. This mechanism underscores the role of catalyst surface interactions, particularly the adsorption of CO_2 at oxygen sites, in driving the reaction toward efficient methane production.

Another notable associative pathway is the carboxyl pathway (Fig. 5), characterized by the direct involvement of CO_2 in the reaction process. In this mechanism, the chemisorbed CO_2 species are initially transformed into carboxyl intermediates (*COOH).[17] These intermediates then undergo a series of hydrogenation steps, ultimately yielding CH_4 as the final product. Similar to the formate pathway, the carboxyl pathway relies on the direct incorporation of CO_2 into intermediate species, facilitating the conversion process leading to methane production. However, a key distinction lies in the adsorption behavior of CO_2 molecules on the catalyst's surface. In this pathway, CO_2 interacts with the catalyst primarily through its carbon center and subsequently forms carbon monoxide (CO) as an intermediate product during the reaction.

In summary, associative pathways in CO_2 methanation involve the direct participation of CO_2 in forming intermediate species, which are subsequently hydrogenated to produce methane. These mechanisms are distinguished by the integration of CO_2 into the reaction process without its prior dissociation into CO and oxygen species. Gaining a comprehensive understanding of these pathways is crucial for refining catalyst designs and optimizing reaction parameters to improve the efficiency of methane production in CO_2 methanation processes.

2.2. Dissociative pathway

Dissociative pathways in CO_2 methanation are characterized by the initial decomposition of CO_2 into CO and oxygen species, which subsequently participate in methane formation. One of the most extensively investigated dissociative mechanisms is

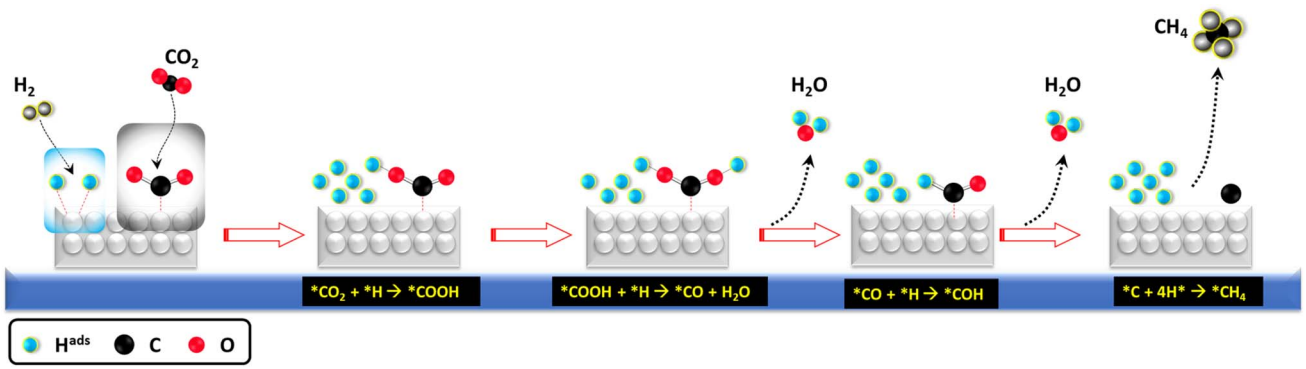

Fig. 5 The carboxyl pathway of CO_2 methanation.

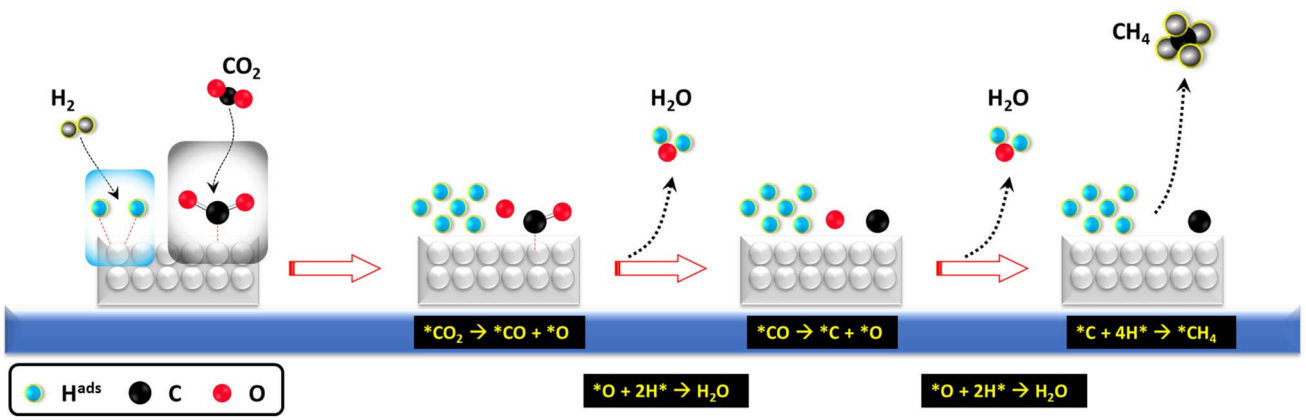

Fig. 6 The dissociative reaction pathway of CO_2 methanation.

the CO pathway, often referred to as CO_2 dissociative methanation. As illustrated in Fig. 6, this pathway involves the chemisorption of CO_2 molecules onto the catalyst's surface, where they break down into *CO and *O intermediates. The *CO species then undergo successive hydrogenation steps, forming carbon species (*C) that further react with hydrogen atoms to generate CH_4. Simultaneously, the *O species combine with hydrogen to form water (H_2O).[18]

3. Technical bottlenecks for implementation of CO_2 methanation

Implementing CO_2 methanation technology is accompanied by several technical challenges that must be addressed to enhance its efficiency and feasibility:

3.1. Catalyst performance

The development of highly active, selective, and stable catalysts is fundamental for the success of CO_2 methanation. A significant challenge lies in optimizing the composition, structure, and active sites of catalysts to achieve high CO_2 conversion rates while minimizing the formation of undesired by-products.[19]

3.2. Low-temperature efficiency

Achieving substantial CO_2 conversion at lower temperatures is vital for improving energy efficiency and reducing operational costs.[20] Enhancing catalytic performance under low-temperature conditions without compromising stability remains a critical issue.

3.3. Catalyst deactivation

Catalyst deactivation due to issues like carbon deposition, poisoning, or sintering can severely impact the efficiency and cost-effectiveness of the process.[21] Strategies to prevent or mitigate these issues, thereby extending the catalyst's lifespan, are urgently needed.

3.4. Reaction kinetics

A deep understanding of the complex reaction kinetics involved in CO_2 methanation is necessary for optimizing both process parameters and reactor design.[22] Identifying and characterizing intermediates and reaction pathways are key to enhancing reaction efficiency and selectivity.

3.5. Hydrogen source

Since CO_2 methanation relies on hydrogen, securing a sustainable and affordable hydrogen supply is paramount. Renewable hydrogen production methods, such as water electrolysis or biogas reforming, should be prioritized to support a viable process.[23]

Addressing these challenges will be instrumental in overcoming these barriers and unlocking the full potential of CO_2 methanation as a solution for carbon capture and utilization.

4. Innovative approaches in catalyst design for CO_2 methanation

Designing catalysts for CO_2 methanation involves a comprehensive approach that integrates the selection of active metals, support materials, nanostructure engineering, active site optimization, reaction condition refinement, and a deep understanding of catalytic mechanisms.[24] These strategies focus on tailoring catalyst properties to enhance CO_2 activation, facilitate H_2 dissociation, and maximize CH_4 production, while simultaneously minimizing the formation of undesired by-products and mitigating catalyst deactivation. Significant progress has been made in developing optimal configurations for heterogeneous catalysts used in CO_2 methanation. These efforts emphasize fine-tuning various components, including active sites, support materials, promoters, and preparation techniques.[25] Among the most promising candidates are metal-oxide-supported catalysts that incorporate active metals, such as noble or transition metals, along with a variety of conventional and advanced support materials.[26,27] In certain cases, interfacial layers or additional promoters, such as secondary metals, are employed to further enhance catalytic performance.[28,29] In the following sections, we delve into the specific modifications and innovations applied to each component of catalytic materials, highlighting their roles in advancing the efficiency and durability of catalysts for CO_2 methanation.

4.1. Factors influencing the performance of heterogeneous catalysts

The efficiency of heterogeneous catalysts in CO_2 methanation is determined by a range of factors that significantly impact their catalytic behavior. A thorough understanding of these factors is crucial for refining catalyst design and improving their effectiveness in CO_2 methanation. As illustrated in Fig. 7, several elements influence the CO_2 methanation performance of metal-based catalysts. These factors are explored in detail in the following sections.

4.1.1. Selection of active metals. In the field of CO_2 methanation, it is essential to differentiate between a catalyst's activity and its selectivity. Earlier research has examined and categorized metal catalysts-primarily from groups 8 to 11 of the periodic table (Fig. 8)-based on their performance in terms of activity and selectivity.[30] These studies often present varying conclusions. However, a careful review and analysis of these studies reveal a consistent trend in the activity and selectivity profiles of different metals used in CO_2 methanation.

Activity:

Ru > Rh > Ni > Fe > Co > Os > Pt > Ir > Mo > Pd > Ag > Au.

Selectivity:

Pd > Pt > Ir > Ni > Rh > Co > Fe > Ru > Mo > Ag > Au.

Based on the published literature, noble metals, such as Ru and Rh, are known for their exceptional activity, while Pd, Pt, and Ir are recognized for their superior selectivity.[31,32] However, their limited availability and high costs pose significant challenges for large-scale industrial use. As a result, there is an increasing focus on identifying cost-effective alternatives with

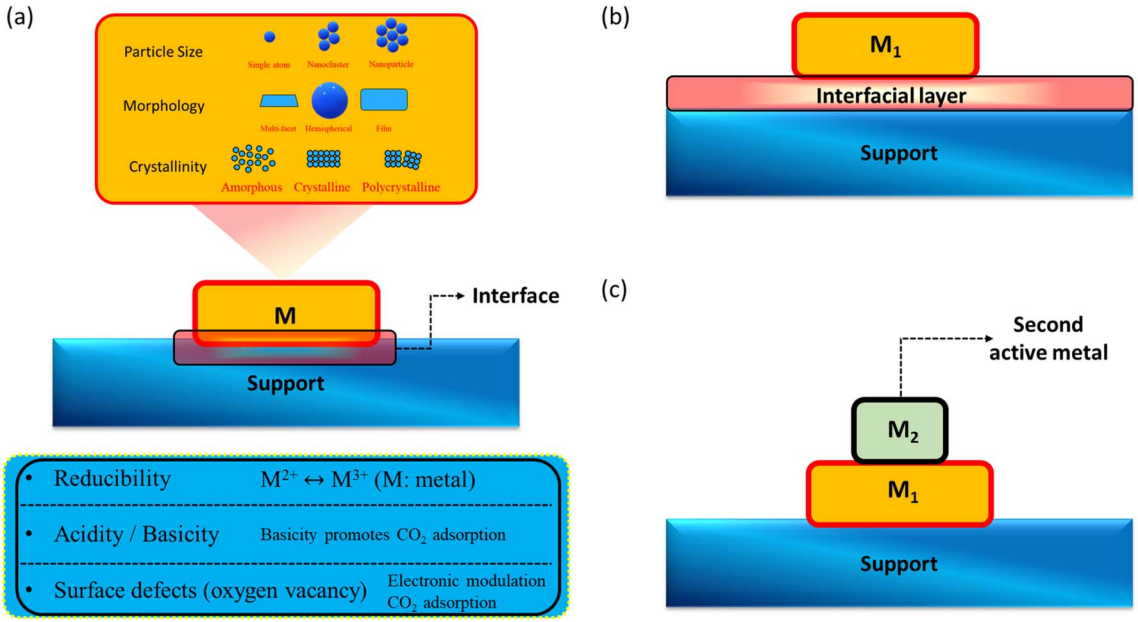

Fig. 7 The schematic representation of factors affecting the catalytic performance of heterogeneous catalysts in CO_2 methanation. Here "M" stands for the active metal. (a) The parameters of active metal affecting the catalytic performance, (b) the interfacial layer and (c) the additive of second metal.

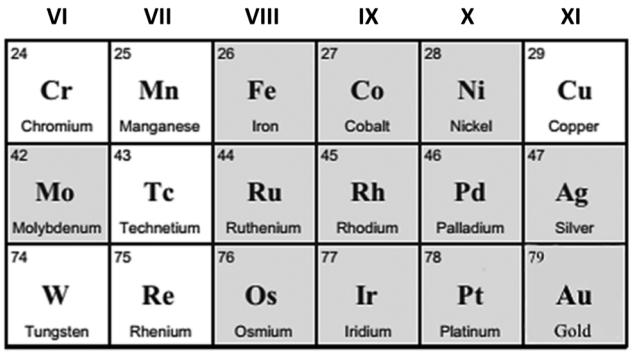

Fig. 8 The elements with shaded portions in the periodic table are active metals for CO_2 methanation.

high catalytic activity. Among these, transition metal-based catalysts supported on metal oxides have gained substantial attention. Nickel (Ni)-based catalysts, in particular, are widely studied for CO_2 methanation due to their excellent catalytic performance and abundant availability.[33,34] Supported Ni nanoparticles, often dispersed on metal oxides, have demonstrated impressive efficiency in CO_2 methanation processes. Some of the Ni-based catalysts exhibited very high activity in the CO_2 methanation with nearly 100% CH_4 selectivity are summarized in Table 1.

While these catalysts have demonstrated significant potential for CO_2 methanation in practical applications, several challenges remain. Issues such as high activation temperatures, limited CH_4 productivity at lower temperatures, and catalyst deactivation due to sintering under reaction conditions pose barriers to their large-scale implementation. Cobalt (Co)-based catalysts exhibit methanation activity comparable to Ni-based catalysts; however, their higher cost makes them less favorable for industrial use. Similarly, iron (Fe)-based catalysts show reasonable activity for CO_2 methanation but suffer from low

Table 1 The CO_2 methanation performance of Ni-based catalysts on metal-oxide supports

Catalyst	Temp (°C)	CO_2 conversion (%)	CH_4 selectivity (%)	References
15 wt% Ni/TiO_2	260	96	99	35
15 wt% Ni–La/SiC	360	85	100	36
10 wt% Ni/CeO_2	350	93	100	37
70 wt% Ni/SBA-15	300–450	99.2	100	38
20 wt% Ni/H–Al_2O_3	300	99	99	39
20 wt% Ni/nanocrystalline γ-Al_2O_3	350	78	100	40
14 wt% Ni/USY	400	65.5	94.2	41
5 wt% Ni/2 wt% ceria/Al_2O_3	300	70	100	42
10 wt% Ni/β-zeolite	360	97	N/A	43
10 wt% Ni/β-zeolite with plasma	240	94	N/A	
12 wt% Ni/ZrO_2–Al_2O_3	360	69.8	100	44
5 wt% Ni–$Ce_xZr_{1-x}O_2$	350	80	98	45

Table 2 Summary of the optimized parameters of the active metals in Ni-based catalysts for enhanced CO_2 methanation

Factors	Catalyst type	Key findings	References
Different Ni–metal loadings	Ni/F-SBA-15	(1) CO_2 methanation was highly influenced by Ni loadings (1–10%) onto F-SBA-15 (2) The CO_2 methanation performance is progressively improved when Ni loading is increased from 1% to 5% Ni and suppressed after further raising the Ni to 10% (3) The XRD results show that the increasing Ni loading from 1 to 5% → NiO crystallite size slightly increased from 7.99 nm to 8.92 nm → representing homogenous dispersion of NiO crystallites. Besides for 10% Ni, a drastic enlargement of NiO crystallites size (17.73 nm) is observed → aggregation	47
Different sizes of Ni nanoparticles with the same metal loading	Ni/CeO_2	(1) The effect of Ni particle size on CH_4 production has been revealed on Ni/CeO_2 catalysts (2) AP-XPS investigation shows that oxygen vacancies are insensitive to Ni particle size (3) The DRIFTS studies revealed that the larger Ni (8 nm particles) over CeO_2 efficiently facilitated the hydrogenation of the surface formate intermediates	48
Different synthesis methods	Ni/Al_2O_3	(1) Al_2O_3-supported Ni nanoparticles are prepared by impregnation method ($NiAl_2O_3$-I) and microwave-assisted ($NiAl_2O_3$-M) methods (2) Ni–Al_2O_3 catalysts prepared by microwave-assisted method show better Ni dispersion and CO_2 methanation performance	49

CH_4 selectivity, limiting their effectiveness.[46] Given these challenges, Ni-based catalysts are considered the most promising for practical and scalable applications. Overcoming the limitations associated with Ni-based catalysts is crucial to fully exploit their potential and support the widespread adoption of metal-oxide-supported Ni-transition metal catalysts in CO_2 utilization technologies. Table 2 provides a summary of key factors optimized in previous studies to enhance the performance of Ni-based catalysts for CO_2 methanation.

4.1.2. Synthesis methodologies. The synthesis method of Ni-based catalysts plays a critical role in determining their physicochemical properties, including surface area, metal dispersion, reducibility, and metal–support interactions, all of which directly impact catalytic performance in CO_2 methanation. For instance, Song *et al.* employed a microwave-assisted synthesis approach to fabricate Ni/Al_2O_3 catalysts (Ni20–Al_2O_3-M), leveraging the efficiency of microwave heating for achieving high dispersion of metal precursors on the support material.[49] To enhance the dispersibility of Ni nanoparticles on γ-Al_2O_3, polyvinyl pyrrolidone (PVP) was introduced as a surfactant, while distilled water acted as a microwave absorbent during the synthesis process. For comparison, a reference catalyst (Ni20–Al_2O_3-I) was prepared using the conventional impregnation method. Structural and morphological characterization techniques, including X-ray diffraction (XRD), Raman spectroscopy, and high-resolution transmission electron microscopy (HRTEM), confirmed that the microwave-assisted method led to superior Ni dispersion. Additionally, H_2-temperature programmed reduction (H_2-TPR) and CO_2-temperature programmed desorption (CO_2-TPD) analyses demonstrated that Ni20–Al_2O_3-M exhibited an increased number of active Ni sites under lower H_2 pretreatment temperatures and improved surface basicity. As a result, Ni20–Al_2O_3-M displayed significantly enhanced catalytic activity for CO_2 methanation, particularly at lower reaction temperatures, while maintaining high CH_4 selectivity across the entire temperature range. Moreover, the catalyst exhibited excellent stability during a 72 hours continuous operation at 325 °C, demonstrating its potential for long-term application in CO_2 methanation processes. Several widely used techniques have been developed to prepare Ni-based catalysts, each offering distinct advantages in optimizing catalyst structure and activity.

Impregnation is one of the most common methods for synthesizing Ni-based catalysts due to its simplicity and scalability. In this method, a porous support material such as Al_2O_3, SiO_2, or CeO_2 is impregnated with a nickel precursor solution (*e.g.*, $Ni(NO_3)_2 \cdot 6H_2O$) followed by drying and calcination.[50] The loading of Ni can be controlled by adjusting precursor concentration, while post-synthetic treatments such as reduction influence metal dispersion and catalyst stability.

Co-precipitation is another widely employed technique that enables uniform mixing of metal precursors and support materials. In this approach, Ni salts and support precursors are simultaneously precipitated from solution using a base such as NaOH or NH_4OH, followed by filtration, drying, and calcination.[51] The advantage of co-precipitation lies in its ability to produce well-dispersed and homogeneously distributed metal nanoparticles, which enhance catalytic activity by providing more accessible active sites.

Sol–gel synthesis is a method that allows for the fine control of metal–support interactions at the molecular level. This process involves the formation of a colloidal solution (sol) that undergoes gelation, drying, and calcination to yield highly porous catalysts with uniform metal dispersion.[52] The sol–gel technique is particularly beneficial for incorporating Ni into

mixed metal oxides, such as Ni–Al_2O_3 or Ni–CeO_2, which exhibit enhanced reducibility and oxygen mobility.

Hydrothermal and solvothermal methods have gained attention for synthesizing Ni-based catalysts with controlled morphology and crystallinity. These techniques involve the reaction of metal precursors in aqueous (hydrothermal) or organic (solvothermal) solutions at elevated temperatures and pressures, leading to the formation of nanostructured catalysts with tailored properties. The hydrothermal approach is particularly useful for preparing Ni catalysts supported on metal oxides with high surface area and strong metal–support interactions, thereby improving catalytic stability.[53]

Deposition–precipitation is another synthesis method that enables precise control over Ni particle size and dispersion. In this technique, Ni precursors are deposited onto a support material through controlled precipitation, followed by washing, drying, and calcination. Compared to traditional impregnation methods, deposition–precipitation provides better metal dispersion and stronger metal–support interactions, which enhance catalytic performance in CO_2 methanation.[54]

Each of these synthesis techniques influences the structural, textural, and electronic properties of Ni-based catalysts, ultimately affecting their efficiency in CO_2 methanation. By selecting an appropriate synthesis method and optimizing reaction conditions, researchers can develop catalysts with improved activity, stability, and resistance to deactivation, making Ni-based catalysts a promising choice for large-scale CO_2 conversion applications.

4.1.3. Selection of support materials. The selection of support materials is a critical factor influencing the performance of Ni-based catalysts in CO_2 methanation.[55] Support materials (*e.g.*, carbon-based materials, metal-oxides, mixed-metal oxides *etc.*) serve as a structural framework for anchoring active metal nanoparticles, aiding their dispersion and impacting the catalyst's surface characteristics. In addition, to conventional supports, zeolite-based nanomaterials have also been used as support material.[56] Several aspects highlight the importance of support materials in optimizing the performance of Ni-based catalysts for CO_2 methanation:

4.1.3.1. Surface area and dispersion. High-surface-area support materials promote uniform dispersion of Ni particles, enhancing interactions between the active metal species and CO_2 molecules. This results in improved catalytic activity and selectivity for methane production.[57]

4.1.3.2. Redox properties. Supports with redox-active sites, such as CeO_2, ZrO_2, and TiO_2, facilitate CO_2 activation and subsequent hydrogenation. These properties enhance the reducibility of Ni species, improving CO_2 conversion efficiency.[58]

4.1.3.3. Acid–base properties. Since CO_2 is acidic, basic support materials are advantageous for its activation, making the catalyst more effective.[59]

4.1.3.4. Metal–support interaction (MSI). Metal–support interaction (MSI) plays a crucial role in determining the activity, stability, and selectivity of heterogeneous catalysts. In CO_2 methanation, MSI influences the electronic structure, dispersion, and oxidation state of the active metal sites, thereby affecting their catalytic performance. Strong metal–support interactions (SMSI) can enhance catalytic activity by facilitating charge transfer between the metal and support, promoting the formation of active sites, and improving resistance to sintering and deactivation. For example, in Ni/CeO_2 catalysts, ceria provides oxygen vacancies that enhance CO_2 adsorption and activation, while Ru/TiO_2 systems benefit from electron transfer effects that modify reaction pathways.[60,61] Understanding and optimizing MSI through advanced techniques such as Density Functional Theory (DFT) and *in situ* spectroscopy is essential for designing high-performance catalysts for thermal and photocatalytic CO_2 conversion. A strong interaction between the Ni species and the support material enhances catalyst stability by reducing metal sintering under reaction conditions. This interaction also affects the electronic structure of the active sites, thereby influencing the overall catalytic activity.[62]

4.1.3.5. Surface oxygen vacancies. Certain support materials, like CeO_2 and TiO_2, contain surface oxygen vacancies that promote CO_2 activation. These vacancies facilitate the generation of reactive oxygen species, which play a key role in methane production.[63]

Table 3 provides an overview of the support materials investigated in previous studies, along with their impact on the performance of Ni-based catalysts.

4.1.4. Interface engineering. Interface engineering in Ni-based catalysts for CO_2 methanation focuses on optimizing the interaction between the active Ni sites and the support material at their interface.[70] This approach aims to improve catalytic performance by regulating factors such as the electronic structure, surface morphology, and chemical environment. Several strategies are employed to achieve effective interface engineering:

4.1.4.1. Selection of support. The choice of an appropriate support material is fundamental for interface optimization. Materials like TiO_2, CeO_2, and Al_2O_3 are commonly used due to their ability to stabilize and disperse Ni nanoparticles, as well as their high surface area and excellent thermal stability.

4.1.4.2. Support modification. Modifying the surface of the support material introduces specific functionalities or defects that enhance the interaction between Ni and the support. Techniques include creating oxygen vacancies, adding dopants, or incorporating functional groups on the surface.

4.1.4.3. Nano-structuring. Designing the nanostructure of both the Ni catalyst and the support material increases the interfacial contact area and facilitates mass transport of reactants and products. Methods such as nanoscale alloying, deposition of nanostructures, or forming hierarchical structures can be employed for this purpose.

4.1.4.4. Tuning electronic properties. Adjusting the electronic properties at the catalyst–support interface can influence the adsorption and activation of CO_2 and H_2 molecules. This can involve modifying the oxidation state of Ni, introducing electron-rich species at the interface, or inducing metal–support interactions that alter the electronic structure of Ni.

4.1.4.5. Synergistic effects. Leveraging synergistic interactions between Ni and the support material can improve both catalytic activity and selectivity. Examples include facilitating

Table 3 Various support materials explored in the published literature

Factors	Catalyst type	Key findings	References
Single metal-oxide support	Ni-based catalysts supported on TiO_2, Al_2O_3, Y_2O_3, and CeO_2	(1) Honeycomb-type Ni-based catalysts with different oxide supports were synthesized (2) 10 wt% Ni/CeO_2 honeycomb catalyst showed the best CO_2 methanation activity (80%)	64
	Ni/ZrO_2	(1) The obtained Ni/ZrO_2 catalyst shows high Ni dispersion with principally exposed Ni(111) lattice plane (2) An enhanced cooperation between Ni and interfacial active sites is achieved as well, which leads to rapid dissociative adsorption of H_2 and hydrogen spillover (3) Sufficient H atoms are thereby generated for CO_2 hydrogenation and helpful in creating oxygen vacancies on the ZrO_2 surface	65
Composite metal-oxide supports	Ni–$Ce_xZr_{1-x}O_2$	(1) Carbon dioxide methanation was carried out over a series of Ni–$Ce_xZr_{1-x}O_2$ catalysts prepared by a pseudo sol–gel method (2) The influence of CeO_2/ZrO_2 mass ratio and noble metal addition was investigated (3) The addition of ZrO_2 to CeO_2 increased the oxygen mobility in the lattice of cerium oxide and promoted the formation of vacancies, which in turn affected the consumption of H_2 and the activation of CO_2 rapidly	45
	NiO/ZrO_2/Al_2O_3	(1) Promotion of the stability, anti-carbon deposition and anti-sintering performance of Ni/Al_2O_3 catalyst modified by ZrO_2 is obtained (2) Adding ZrO_2 restrains the formation of $NiAl_2O_4$, weakens the Ni–Al_2O_3 interaction, and makes the catalyst more easily reduced, enhancing significantly the activity of catalyst	66
Carbon supports	Ni/Ce–CNT	(1) The confinement effect of carbon nanotubes prevented the active phase migration and sintering (2) Catalytic performances exhibited that Ni/Ce–CNT catalyst possessed the highest activity with 83.8% conversion of CO_2 and almost 100% selectivity of CH_4 without obvious deactivation after a 100 h stability test under reaction conditions	67
	Ni–Ce/RGO	(1) The oxygen functional groups can act as anchoring sites to improve the dispersion of nickel nano-particles on RGO (2) The Ni–Ce/RGO works the best for CO_2 methanation, which could reach the highest CO_2 conversion of 84.5% and the highest methane yield of 83.0% at 350 °C with atmospheric pressure as compared to Al_2O_3 support	68
Zeolite supports	Ni catalysts on ITQ-2 and ZSM-5 zeolites support	(1) The higher hydrophobicity of used zeolites favors the CO_2 methanation	69

the spillover of reactive intermediates between Ni and the support or developing dual-function sites for CO_2 activation and hydrogenation.

One of the notable example of interface engineering has been reported by Zhou *et al.*, where they controlled the metal support interaction between Ru and TiO_2 *via* proper controlling the interfacial compatibility.[71] Given that the nature of the support material significantly influences the catalytic activity, selectivity, and stability of metal nanoparticles, primarily through metal–support interactions (MSIs). However, the intricate mechanisms governing these interactions remain incompletely understood, as MSIs are affected by factors such as the composition, size, and crystallographic facets of both the metal and the support. Utilizing Ru/TiO_2 catalysts supported on rutile and anatase as model systems, it has been shown that interfacial compatibility plays a decisive role in controlling MSI modes and catalytic behavior in CO_2 hydrogenation. When Ru/rutile-TiO_2 is annealed in air, the resulting improved interfacial coupling, driven by lattice matching between RuO_x and rutile-TiO_2, enhances the conversion of CO_2 to methane. Conversely, annealing Ru/anatase-TiO_2 leads to reduced CO_2 conversion and shifts the reaction product to CO, attributed to the formation of strong metal–support interactions (SMSIs). Despite having the same chemical composition, rutile and anatase exhibit distinct effects on interfacial coupling, demonstrating how compatibility at the interface can profoundly influence the coupling strength, surface morphology, atomic configurations, MSI modes, and overall catalytic performance of Ru/TiO_2 in heterogeneous catalysis. Furthermore, Kang *et al.* demonstrated the effect of interfacial layer between active metal and support for enhanced H-spillover during CO_2 conversion.[72] It is frequently reported in the literature that the migration of reducible metal oxides, such as TiO_2, onto the surface of metal nanoparticles can help prevent sintering but often negatively

affects catalytic activity. However, a novel approach demonstrates the *in situ* formation of TiO_x patches on an MnO support, creating effective pathways for hydrogen spillover. These pathways facilitate the generation of highly active hydrogen species on the MnO surface, which are crucial for converting CO_2 to CO—a pivotal step in transforming CO_2 into valuable chemicals. The Ru/(TiO_x)MnO (Ru/Ti/Mn) catalyst exhibits a 3.3-fold improvement in reverse water–gas shift (RWGS) performance compared to traditional Ru/MnO_x catalysts. Using a combination of advanced techniques, including *in situ* analyses, kinetic and catalytic evaluations, and theoretical modeling, it has been shown that the oxide–oxide interfaces, formed spontaneously during reductive treatment in H_2, significantly enhance catalytic activity. This finding underscores the potential of designing innovative hydrogenation catalysts by leveraging *in situ* oxide–oxide interface creation as active transport channels for hydrogen species. Another interesting study on the importance of interface has been demonstrated by Xu *et al.*, where a highly efficient composite Ni–Y_2O_3 catalyst was developed, demonstrating exceptional performance by forming numerous active Ni–NiO_x–Y_2O_3 interfaces under water–gas shift (WGS) reaction conditions.[73] This catalyst achieved a remarkable activity rate of 140.6 $\mu mol_{CO}\ g_{cat}^{-1}\ s^{-1}$ at 300 °C, marking it as the most active Ni-based catalyst to date. Through a combination of theoretical analysis and *ex*/*in situ* experimental studies, it was revealed that Y_2O_3 plays a crucial role in facilitating H_2O dissociation at the Ni–NiO_x–Y_2O_3 interfaces, effectively accelerating this rate-limiting step in the WGS reaction. The creation of such innovative interfacial structures for molecular activation highlights significant potential for advancing catalytic systems in various applications. In summary, interface engineering for Ni-based catalysts aims to finely tune the properties of both the active metal sites and the support material to create highly efficient and selective systems for converting CO_2 into methane. Table 4 highlights significant examples of interface engineering strategies applied to Ni-based catalysts for CO_2 methanation.

4.1.5. Addition of secondary metals. Researchers have extensively investigated the role of transition metal additives in improving the performance of Ni-based catalysts for CO_2 methanation. Among these, Fe and Co are frequently highlighted as effective secondary metals. The incorporation of such dopants into the Ni lattice can significantly alter the electronic properties of nickel and influence the methanation reaction

Table 4 Notable examples of interface engineering

Factors	Catalyst type	Key findings	References
Interface engineering	Ni/ZrO_{2-x}	(1) Zirconium dioxide-supported Ni catalysts toward low-temperature CO_2 methanation are obtained *via* structural topological transformation of NiZrAl-layered double hydroxide (LDH) precursors, which have the feature of an interfacial structure (Ni–O–Zr^{3+}–Vö) between Ni nanoparticles and ZrO_{2-x} support ($0 < x < 1$) (2) The optimized catalyst (Ni/ZrO_{2-x}–S_2) exhibits exceptional CO_2 conversion (~72%) at 230 °C temperature with ~100% CH_4 selectivity	74
	Ni/$mpCeO_2$	(1) Ni nanoparticles were encapsulated in ordered mesoporous ceria, $mpCeO_2$, for CO_2 methanation (2) At 225 °C, TOF of Ni/$mpCeO_2$ catalyst (0.183 s^{-1}) is 3 times higher than Ni catalyst supported on conventional CeO_2 prepared by the same method (0.057 s^{-1}) (3) The encapsulated structure provides a rich Ni–CeO_2 interface with more oxygen vacancies, playing a key role in CO_2 activation (4) Small and highly dispersed Ni nanoparticles in channels of $mpCeO_2$ facilitate H_2 dissociation	75
	Ni–NiO_x–Y_2O_3	(1) The cross-referencing results of *ex*/*in situ* experimental study and theoretical calculations indicates that Y_2O_3 favors the H_2O dissociation at the Ni–NiO_x–Y_2O_3 interfaces	73
	Ru/TiO_2	(1) The results show that rutile and anatase TiO_2 supports can dramatically modify the morphology, surface atomic configuration, MSI mode, and catalytic performances of Ru catalysts for CO_2 hydrogenation reaction, although they share the same chemical compositions (2) Ru/R-TiO_2–H_2 and Ru/A-TiO_2–H_2 show similar CO_2 conversions between 120 °C and 320 °C, suggesting that R-TiO_2 and A-TiO_2 apply similar support effects on directly reduced Ru/TiO_2 catalysts (3) However, the CO_2 conversion efficiency dramatically differentiate by pre-annealing treatment in air at 400 °C. Ru/R-TiO_2–air–H_2 displays an enhanced catalytic performance, with CO_2 conversion at 300 °C increasing from 31.4% to 89.2% (4) Ru/A-TiO_2–air–H_2 shows a highly decreased activity, with CO_2 conversion at 300 °C reducing from 29.4% to 1.7%. At each reaction temperature, Ru/R-TiO_2–air–H_2 shows the highest CO_2 conversions among four catalysts. The results indicate that R-TiO_2 and A-TiO_2 apply opposite support effects on the activity of Ru NPs	71

pathway. These modifications may enhance the catalyst's activity and stability or, in some cases, lead to deactivation, depending on several factors. Key considerations include the ratio of Ni to the dopant, the extent of intermixing between the metals, and the interaction of the metal additives with the support material. By strategically integrating transition metal additives, the catalytic properties of Ni-based systems can be fine-tuned, resulting in improved CO_2 methanation performance. However, achieving the desired outcomes requires a careful balance of these parameters to prevent potential deactivation of the catalyst. Table 5 provides an overview of examples where secondary metal additives have been employed

Table 5 Notable examples of the second metal additives to Ni-based catalysts

Additive	Catalyst type	Key findings	References
Fe	Ni_xFe_{1-x}/Al_2O_3	(1) The maximum carbon conversion and CH_4 selectivity are achieved on $Ni_{0.7}Fe_{0.3}/Al_2O_3$ catalyst, outperforming the monometallic Ni/Al_2O_3 (2) Further, increasing Fe content led to enhancing the water gas shift reaction and hydrocarbon formation	76
	Ni_xFe_y/Al_2O_3	(1) A systematic investigation on Fe promotion in Ni-based methanation catalysts reveals that catalysts comprising 75% Ni and 25% Fe exhibited optimal activity (2) Bimetallic NiFe alloy catalysts supported on alumina and silica displayed higher CH_4 yields compared to their monometallic counterparts (Ni and Fe), with alumina-supported catalysts showing superior enhancement (3) This enhancement was attributed to the formation of a suitable alloy phase and increased CO_2 chemisorption at unreduced Fe_3O_4 sites	77
	NiFe alloy	(1) Fe promotes Al_2O_3, ZrO_2, TiO_2 and SiO_2 supported Ni during CO_2 hydrogenation (2) Enhancement due to the formation of suitable Ni–Fe alloy on all supported catalysts	78
	Ni_3M/Al_2O_3	(1) Ni_3M/Al_2O_3 (M = Fe and Cu) possess different types (Ni_3Fe and $Ni_{1-x}Cu_x$) of alloys (2) Enhanced CO_2 methanation performance over Ni_3Fe catalysts, attributed to favorable changes in the electronic properties of the active Ni phase (3) In contrast, Ni_3Cu alloy formation was found detrimental to CH_4 production	79
	17 wt% Ni_3Fe/γ-Al_2O_3	(1) A γ-Al_2O_3 supported Ni_3Fe alloy catalyst with high dispersion was prepared (24%) (2) A high fraction of Ni and Fe formed the desired Ni_3Fe alloy within a size range of 4 nm (3) As-prepared material outperforms the monometallic counterparts	80
	$Ni_{3.2}Fe/Al_2O_3$	(1) They investigated the deactivation of a Ni-based catalyst and unravelled the protective role of "sacrificial" iron in a $Ni_{3.2}Fe$ catalyst during dynamic CO_2 methanation (2) During the simulated H_2 dropout, the monometallic Ni catalyst was prone to form surface oxygen species resulting in an irreversible formation of NiO leading to catalyst deactivation during the subsequent methanation step (3) In the presence of Fe, the active Ni^0 species was protected from oxidation during the simulated H_2 dropout by preferential formation of FeO	81
	Ni–Fe/(Mg, Al)O_x	(1) The Fe/Ni ratio severely affects the product yield	82
Co	Co-modified Ni/SiO_2	(1) Methanation activities of Ni–Co/SiO_2 catalysts were significantly dependent on Co/Ni molar ratios (2) The increase of Co loading led to the remarkable increase of CO_2 conversions at temperature range from 250 to 350 °C	83
	Co–Ni catalyst on ordered mesoporous Al_2O_3	(1) The synergistic collaboration between Co–Ni decreased the activation energy of CO_2 methanation (2) Ni and Co existed as adjacent monometallic phases on the mesoporous Al_2O_3 structure, serving as active sites for H_2 and CO_2 chemisorption, respectively	84
	Ni–Co/Al_2O_3	(1) The addition of cobalt improved the reducibility of nickel species	85
	Ni–x/CeO_2–ZrO_2 (x = Fe, Co)	(1) Co is an excellent promoter to boost the activity and selectivity towards methane	86

to enhance the efficiency of Ni-based catalysts in CO_2 methanation. More specifically, the role of Fe and Co as promoters in Ni-based catalysts for CO_2 methanation is intricately linked to their influence on reaction pathways, active site modification, and overall catalytic performance. While Fe is known to facilitate CO_2 dissociation, favoring the dissociative pathway, Co is suggested to enhance H_2 activation, promoting the formate and carboxyl pathways. However, a comprehensive understanding of the dominant reaction mechanism and its governing factors remains critical. Systematic experimental validation of these pathways requires an in-depth investigation of the structural and electronic modifications induced by Fe and Co in Ni-based catalysts. Advanced characterization techniques such as *in situ* X-ray photoelectron spectroscopy (XPS), X-ray absorption spectroscopy (XAS), and diffuse reflectance infrared Fourier transform spectroscopy (DRIFTS) can provide valuable insights into electronic interactions, oxidation states, and surface species evolution during CO_2 methanation. Additionally, density functional theory (DFT) calculations coupled with kinetic modeling can aid in establishing a quantitative correlation between the nature of the promoter, CO_2 activation pathways, CO_2 conversion, and CH_4 selectivity. A holistic approach integrating experimental and computational findings is essential to unravel the mechanistic complexities of CO_2 methanation and to optimize catalyst design for enhanced efficiency and selectivity.

4.1.5.1. Promotion of Ni-based catalysts with Fe. Iron (Fe) has emerged as a widely studied secondary metal in bimetallic Ni-based catalysts for CO_2 methanation due to its cost-effectiveness, availability, and its ability to dissolve readily in the Ni lattice to form NiFe alloys (Fig. 9a).[87] Computational studies and experimental data suggest that alumina-supported, Ni-rich NiFe catalysts significantly enhance CO_2 conversion rates, with the ideal Ni/(Ni + Fe) ratio ranging from 0.7 to 0.9.[88,89] Extensive research has been conducted on NiFe alloys

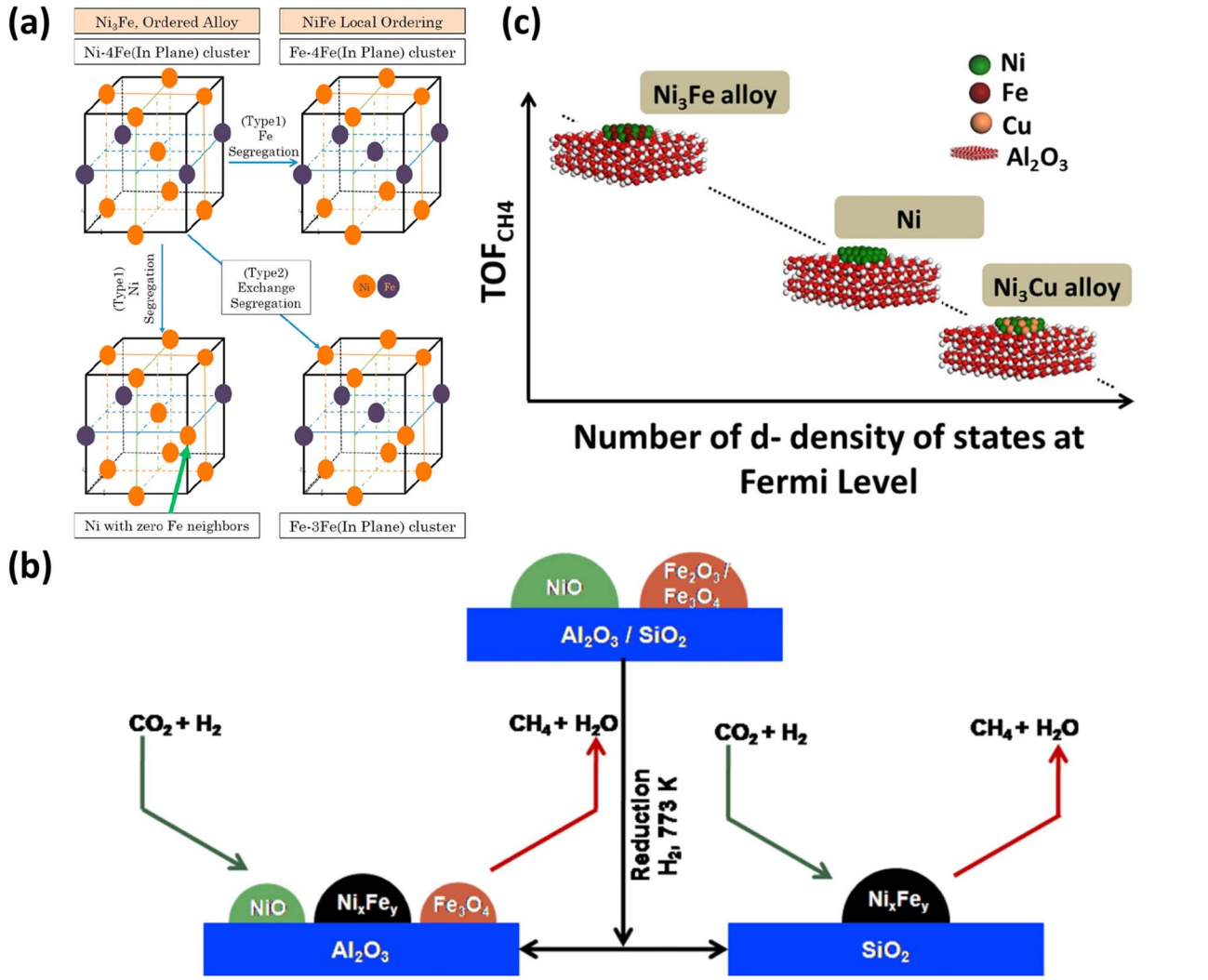

Fig. 9 (a) Solubility of Fe in Ni lattice (this figure has been reproduced from ref. 87 with permission from Elsevier, copyright 2018). (b) Promotional effects in alumina and silica-supported bimetallic Ni–Fe catalysts during CO_2 hydrogenation (this figure has been reproduced from ref. 78 with permission from Elsevier, copyright 2016). (c) Linear correlation between the turnover frequency for CH_4 production ($TOFCH_4$) and the number of d-density of states (d-DOS) at Fermi level (NEF) for Ni, Ni_3Fe and Ni_3Cu catalysts (this figure has been reproduced from ref. 79 with permission from Elsevier, copyright 2017).

synthesized through various techniques and supported on different metal oxides.[78] The Ni/Fe ratio and the reducibility of the support material have been identified as key factors determining whether Fe acts as a promoter or inhibitor for CO_2 methanation activity. In a notable study, Pandey *et al.* systematically explored Fe promotion in Ni-based catalysts, demonstrating that a composition of 75% Ni and 25% Fe delivered optimal catalytic performance.[90] Bimetallic NiFe alloy catalysts supported on alumina and silica exhibited higher methane yields compared to their monometallic counterparts, with alumina-supported catalysts showing the greatest improvement (Fig. 9b). This enhanced activity was attributed to the formation of favorable alloy phases and improved CO_2 chemisorption at unreduced Fe_3O_4 sites. Further investigation into Ni_3Fe catalysts on various supports identified alumina as the most effective due to its interaction with Fe, which enhanced alloy formation and catalytic performance.[78] In another study, Ray *et al.* developed a predictive model for CO_2 methanation performance in Ni_3M bimetallic catalysts, where M represents Fe or Cu. Using density functional theory (DFT) calculations, they correlated the turnover frequency for methane production ($TOF\text{-}CH_4$) with the density of d-states (d-DOS) at the Fermi level (Fig. 9c). This model confirmed enhanced methanation performance for Ni_3Fe catalysts due to favorable modifications in the electronic properties of the active Ni phase. Conversely, the formation of Ni_3Cu alloys was found to inhibit methane production.[79]

The Grunwaldt group has significantly advanced the development of NiFe-based methanation catalysts, offering valuable insights into the role of Fe in enhancing catalytic performance. In one study, Mutz *et al.* synthesized Ni_3Fe catalysts supported on Al_2O_3 through a deposition–precipitation method.[91] The resulting alloy nanoparticles were highly dispersed and exhibited small sizes, resulting in superior activity and stability at lower temperatures compared to monometallic Ni-based catalysts. Notably, these catalysts demonstrated stable performance over a 45 hours time-on-stream operation under industrially relevant conditions, with no evidence of carbon deposition under various gas feeds, as revealed by *operando* Raman spectroscopy. This finding underscored the durability and resistance to deactivation of the NiFe alloy catalysts. Farsi *et al.* investigated the kinetics of CO_2 methanation using Ni_3Fe catalysts under practical operational conditions. Their study found that shorter residence times and elevated temperatures led to increased CO selectivity over CH_4, with water concentration acting as a significant inhibiting factor.[92] Furthering this work, Serrer *et al.* employed advanced *operando* spectroscopic techniques to explore Fe's role in CO_2 methanation.[81] They discovered that Fe acts as a "sacrificial" dopant, particularly under H_2-dropout conditions during methanation (Fig. 10a). Unlike Ni-based catalysts, which undergo oxidation and fail to recover their initial activity when H_2 flow is restored, NiFe-based catalysts maintain reduced Ni^0 sites due to Fe's preferential oxidation to FeO. Under normal operating conditions, Fe enhances the reducibility of Ni, leading to the formation of small FeO_x clusters on the surface of alloy nanoparticles. These clusters, exhibiting various oxidation states, are believed to promote CO_2 chemisorption and activation, potentially contributing to the increased methanation performance of NiFe alloy catalysts (Fig. 10b). This protective and enhancing role of Fe provides a mechanistic basis for the superior performance of NiFe-based systems in CO_2 methanation.[93]

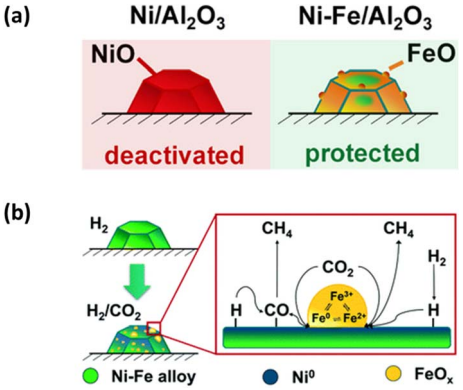

Fig. 10 (a) Deactivation of a monometallic Ni-based catalyst and the protective role of "sacrificial" iron in a NiFe catalyst during dynamic methanation of CO_2 (this figure has been reproduced from ref. 81 with permission from Wiley, copyright 2019). (b) Scheme representation of the CO_2 activation mechanism on Ni–Fe alloy-based catalysts during methanation reaction (this figure has been reproduced from ref. 93 with permission from RSC, copyright 2020).

Mebrahtu *et al.* developed NiFe/(Mg, Al)O_x catalysts using hydrotalcite precursors with a tailored Fe/Ni ratio to achieve high metal dispersion and intermixing.[82] The Fe/Ni ratio played a critical role in shaping the catalysts' physicochemical characteristics and catalytic performance. Notably, an Fe/(Ni + Fe) ratio of 0.1 was found to optimize key parameters, including nanoparticle size, metal dispersion, and the presence of surface basic sites. Catalysts with this composition demonstrated exceptional low-temperature performance, achieving high CO_2 conversion and CH_4 selectivity, outperforming those with higher Fe content, as depicted in Fig. 11. The study also highlighted a potential deactivation mechanism in monometallic Ni catalysts, wherein the *in situ* generation of water during the

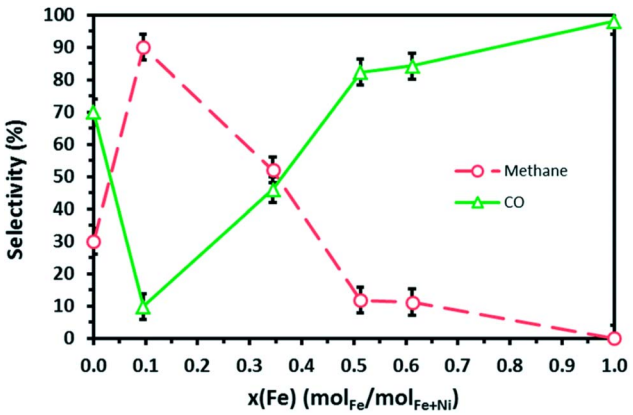

Fig. 11 Effect of Fe content on CH_4 and CO selectivity in comparison to sole metals (this figure has been reproduced from ref. 82 with permission from RSC, copyright 2018).

methanation process leads to the formation of Ni hydroxides. Mebrahtu *et al.* also observed that the inclusion of Fe mitigated this deactivation pathway by suppressing the formation of Ni–OH species, thereby enhancing the catalyst's stability and activity.[94] Additionally, it was proposed that Fe, instead of forming alloys with Ni, contributed to spinel phase formation on alumina nanosheets. This strategic incorporation of Fe not only prevented deactivation but also augmented the overall catalytic efficiency of the NiFe/(Mg, Al)O_x system. These findings underscore the significance of precise Fe/Ni ratio optimization in enhancing the performance of Ni-based catalysts for CO_2 methanation.

Furthermore, the research has explored the influence of Fe addition on the performance of Ni-based catalysts, revealing varied results depending on the catalyst composition, support material, and Fe loading. For instance, Li *et al.* reported that introducing 3% Fe to a 12% Ni/Al_2O_3 catalyst slightly improved CO_2 conversion and CH_4 selectivity. However, increasing the Fe content to 12% (Fe/Ni $\approx$ 1) resulted in reduced methanation efficiency (Fig. 12a).[95] Liang *et al.* investigated Fe-modified Ni/Al_2O_3 catalysts and observed an increase in oxygen vacancies, altering the reaction mechanism as confirmed by electron paramagnetic resonance (EPR).[96] Conversely, Daroughegi *et al.* found that a 25% Ni/Al_2O_3 catalyst with 5% Fe performed worse than its monometallic Ni counterpart in methanation activity.[97] The choice of support material also plays a significant role in the methanation performance of NiFe-based catalysts.[98] Ren *et al.* demonstrated that modifying a 30% Ni/ZrO_2 catalyst with 3% Fe improved its low-temperature activity.[99] However, higher Fe contents led to decreased performance due to the incomplete reduction of Fe species, which remained in the Fe(II) oxidation state (Fig. 12b). These Fe(II) species enhanced Ni dispersion and reducibility and promoted the reduction of ZrO_2, creating oxygen vacancies that facilitated CO_2 chemisorption and dissociation (Fig. 12c). Yan *et al.* studied low-load Ni and Fe catalysts supported on ZrO_2 and identified distinct interfacial sites that influenced product selectivity during CO_2 hydrogenation.[100] Adding Fe in an equimolar ratio to Ni slightly improved CO_2 conversion and CH_4 selectivity by maintaining a methane-selective Ni–ZrO_2 interface. However, a high Fe/Ni ratio (Fe/Ni = 3) increased CO selectivity by favoring the reverse water–gas shift (RWGS) reaction through the formation of Ni–FeO_x interfaces. Other investigations highlighted the role of Fe promotion in enhancing the methanation performance of Ni-based catalysts supported on Al_2O_3 and mesoporous clay modified with ZrO_2.[101,102] These findings underline the complex relationship between catalyst composition, support material properties, and operating conditions, which collectively dictate the effectiveness of CO_2 methanation.

4.1.5.2. Promotion of Ni-based catalysts with Co. Cobalt (Co), a transition metal similar to nickel (Ni), is widely utilized in bimetallic NiCo catalysts for CO_2 methanation. Its ability to integrate into the Ni lattice and transition between oxidation states (Co^{3+}, Co^{2+}, and Co^0) enables modifications to the electronic properties of the catalyst.[103] Early investigations by Guo *et al.* examined SiO_2-supported NiCo catalysts with varying Co/Ni ratios, finding that higher Co content enhanced catalytic activity, with an optimal Co/Ni ratio of 0.4.[46] The formation of a uniform NiCo alloy facilitated CO dissociation and hydrogen spillover, improving methanation performance.[83] Subsequent research shifted focus to Al_2O_3-supported NiCo catalysts, employing methods like evaporation-induced self-assembly

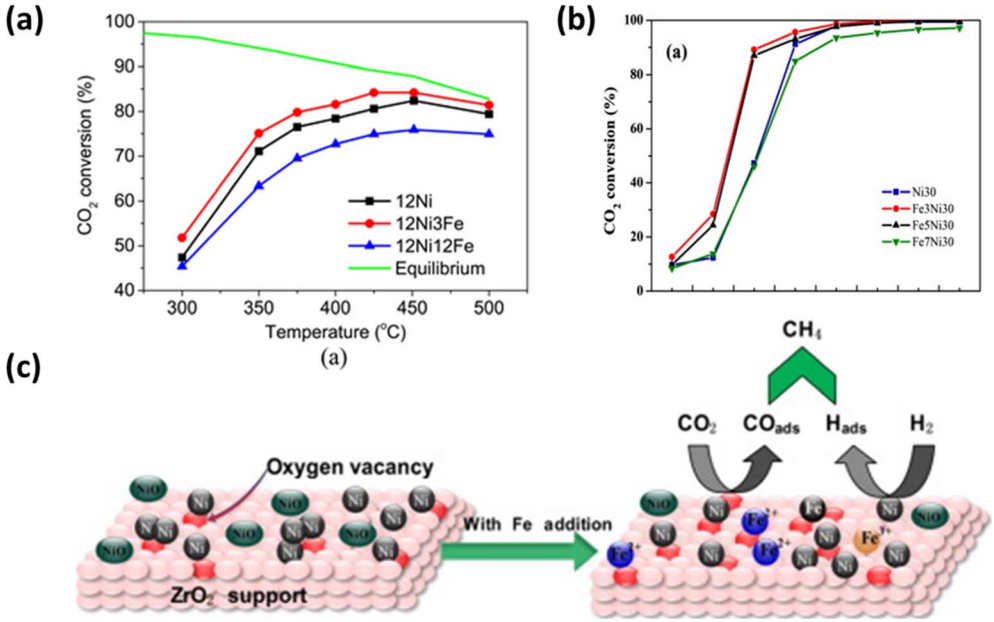

Fig. 12 (a) The CO_2 conversion performance of NiFe catalysts with different Fe content (this figure has been reproduced from ref. 95 with permission from Wiley, copyright 2018). (b) CO_2 conversion over Ni–Fe/ZrO_2 catalysts with various Fe content (this figure has been reproduced from ref. 99 with permission from Elsevier, copyright 2019), and (c) schematic representation of CO_2 methanation over Ni/ZrO_2 and NiFe/ZrO_2 (this figure has been reproduced from ref. 100 with permission from Elsevier, copyright 2015).

(EISA) to introduce ordered mesoporosity. Xu *et al.* demonstrated that a Co/(Ni + Co) ratio of 20% improved catalytic activity and stability, attributing the enhancement to the synergy between Ni and Co phases, which served as active sites for H_2 and CO_2 chemisorption, respectively (Fig. 13a and b). This interaction reduced the activation energy for CO_2 methanation.[84] Similarly, Liu *et al.* reported improved low-temperature activity and stability in ordered mesoporous $NiCo/Al_2O_3$ composites due to NiCo alloy formation and the confinement effect of the mesoporous structure.[104] Alrafei *et al.* studied Al_2O_3-supported NiCo catalysts and observed that a bimetallic catalyst with 10% Ni and 10% Co outperformed a monometallic 10% Ni catalyst, as Co enhanced the dispersion and reducibility of Ni.[105] However, a monometallic 20% Ni catalyst surpassed the performance of bimetallic catalysts with a total metal loading of 20%. All tested catalysts exhibited excellent stability over 200 hours of operation.[49] Conversely, Fatah *et al.* found that adding 5% Co to a 5% Ni/Al_2O_3 catalyst reduced CO_2 conversion and CH_4 selectivity by approximately 30%, likely due to the formation of larger particles and an increased presence of formate intermediates.[106] Beyond SiO_2 and Al_2O_3, research has focused on other supports like ZrO_2 and CeO_2-based materials. Ren *et al.* showed that modifying 30% Ni/ZrO_2 catalysts with Co enhanced CO_2 conversion but slightly reduced CH_4 selectivity compared to Fe-modified counterparts.[99] Razzaq *et al.* demonstrated that Co-modified Ni/CeO_2–ZrO_2 catalysts were particularly effective for CO and CO_2 co-methanation in CH_4-rich gas mixtures.[107] Zhu *et al.* confirmed that adding 5% Co to 15% Ni/CeO_2–ZrO_2 catalysts improved activity and stability for CO_2 methanation.[108] Pastor-Pérez *et al.* also reported that a 3% Co addition enhanced CO_2 conversion, CH_4 selectivity, long-term stability, and coke resistance.[86] In other studies, defect-rich supports like GDC did not show improved catalytic performance with Co promotion. Jia *et al.* utilized TiO_2-coated silica spheres as supports, with the reducible TiO_2 layer improving metal dispersion and enhancing CO_2 and H_2 adsorption.[109] Zhang *et al.* incorporated Co into $LaNiO_3$ perovskite lattices supported on mesostructured cellular foam silica, yielding catalysts with enhanced activity and stability.[110] In summary, cobalt's addition to Ni-based catalysts generally enhances CO_2 methanation performance by improving Ni reducibility, dispersion, and electronic properties. While the type of support material—whether inert or reducible—has a limited influence on the promotion mechanism, the Co/(Ni + Co) ratio plays a less critical role compared to similar NiFe systems. Overall, Ni-rich NiCo catalysts demonstrate consistently superior activity and stability for CO_2 methanation.

4.1.6. Role of oxygen vacancies for CO_2 methanation performance. Oxygen vacancies are critical in determining the effectiveness of catalysts used in the CO_2 methanation process. These vacancies, which represent defects within the lattice structure of materials like CeO_2, ZrO_2, and their derivatives, serve as active sites for CO_2 activation and subsequent conversion to methane.[111] A deeper understanding of these vacancies can inform strategies for optimizing catalyst design and enhancing performance.

4.1.6.1. CO_2 activation at oxygen vacancies. Oxygen vacancies function as adsorption and activation sites for CO_2 molecules due to their unique electronic characteristics. These defects facilitate the interaction of CO_2 with the catalyst surface, leading to its dissociation into reactive intermediates. This activation step is crucial for initiating the reaction pathway that eventually results in methane production.

4.1.6.2. Redox properties and catalytic cycle. Oxygen vacancies also influence the redox behavior of catalysts. By enabling the exchange of oxygen atoms between the catalyst surface and the reactants, they play an essential role in the methanation

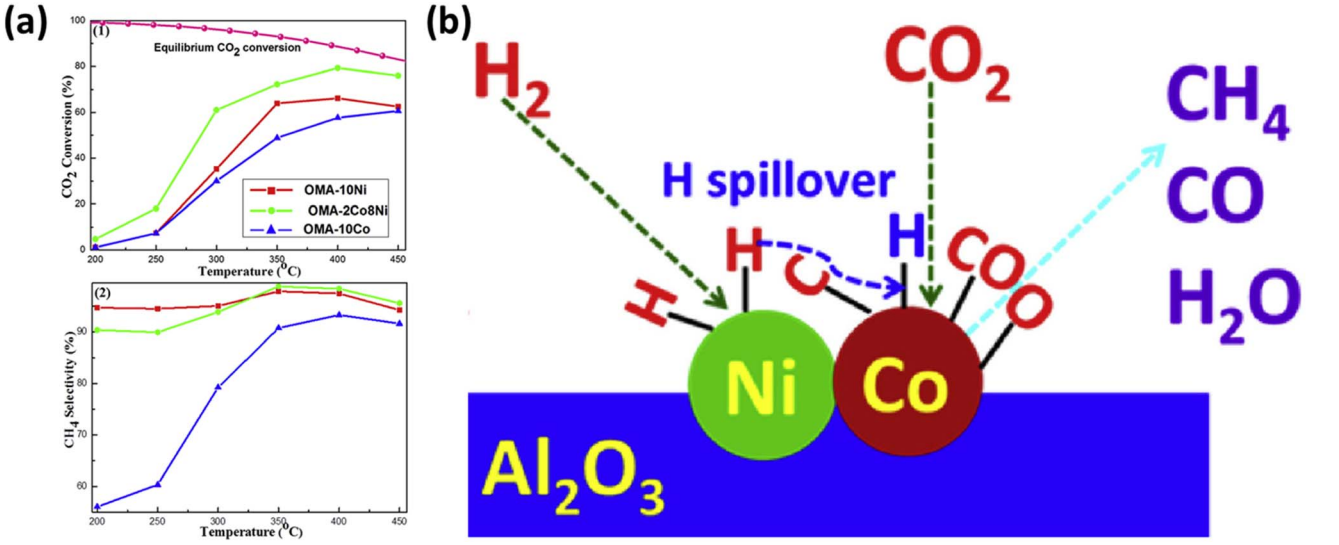

Fig. 13 (a) The CO_2 conversion and CH_4 selectivity *versus* reaction temperature over OMA–10Ni, OMA–2Co8Ni, and OMA–10Co catalysts. (b) The proposed synergistic mechanism between Co and Ni domains over the OMA–*x*Co*y*Ni catalysts toward CO_2 methanation (this figure has been reproduced from ref. 84 with permission from Elsevier, copyright 2018).

cycle. This activity promotes the efficient conversion of CO_2 and H_2 into methane and water.

4.1.6.3. Enhancing stability and longevity. The presence of oxygen vacancies contributes to the stability and durability of catalysts during extended reaction periods. These defects not only provide active sites for CO_2 conversion but also maintain the structural integrity of the catalyst, ensuring consistent performance over time. Stability and resistance to deactivation are essential for practical applications of CO_2 methanation catalysts.

4.1.6.4. Improved metal–support interactions. Oxygen vacancies also affect the dispersion and interaction of active metal sites, such as nickel or cobalt, supported on oxide surfaces. Strong interactions between the metal and the support, mediated by oxygen vacancies, enhance the accessibility and reactivity of the metal sites, thereby improving catalytic efficiency.

4.1.6.5. Case studies. Various researchers have demonstrated the importance of oxygen vacancies for CO_2 methanation. It is frequently reported in the literature that creating oxygen vacancies in metal oxide supports, especially CeO_2, boosts the CO_2 methanation process. For instance, the mechanism of CO_2 methanation was examined for Ni/CeO_2 and Ni/Al_2O_3 catalysts, with Ni/CeO_2 demonstrating superior activity and selectivity.[112] This is attributed to three key factors: (i) Ni/CeO_2 features two distinct active sites, where the NiO–CeO_2 interface facilitates efficient CO_2 dissociation, and Ni^0 particles enhance H_2 dissociation; (ii) water desorption, the rate-limiting step, is expedited by the high oxygen mobility within the ceria lattice, preventing water molecules from occupying CO_2 adsorption sites; and (iii) the Ni/CeO_2 surface resists the buildup of carbon-containing species, enabling continuous CO_2 adsorption and dissociation. Conversely, Ni/Al_2O_3 faces challenges as all reaction steps occur on the same active sites, leading to delayed CO_2 adsorption due to slow water release and the accumulation of surface formats. The reaction pathways for CO_2 methanation on both supports are presented in Fig. 14a. Regardless of the well-explored role of oxygen vacancies in the metal oxide supports, Beniwal *et al.* revealed the merits of oxygen vacancies in the active metal for CO_2 methanation.[14] A novel heterogeneous catalyst, NiFe–TiO_2, featuring oxygen vacancy-enriched atomic Fe-oxide clusters confined within TiO_2-supported Ni-hydroxide, was developed using a wet chemical reduction method (Fig. 14b). This catalyst exhibited exceptional CH_4 productivity of ~24 358 mmol g^{-1} h^{-1} at 300 °C, nearly doubling the performance of Ni–TiO_2 (12 481 mmol g^{-1} h^{-1}) by ~95%. It also demonstrated remarkable durability, achieving a peak productivity of ~36 399 mmol g^{-1} h^{-1} with 90.5% CH_4 selectivity after 116 cycles (155 hours) and maintaining stability over 220 cycles (330 hours). Mechanistic studies revealed that oxygen vacancies in Fe-oxide clusters and adjacent Ni-hydroxide domains synergistically enhance CO_2 activation and H_2 dissociation, enabling efficient methanation kinetics. These findings highlighted the critical role of oxygen vacancies in improving catalytic performance and pave the way for designing advanced catalysts for various applications.

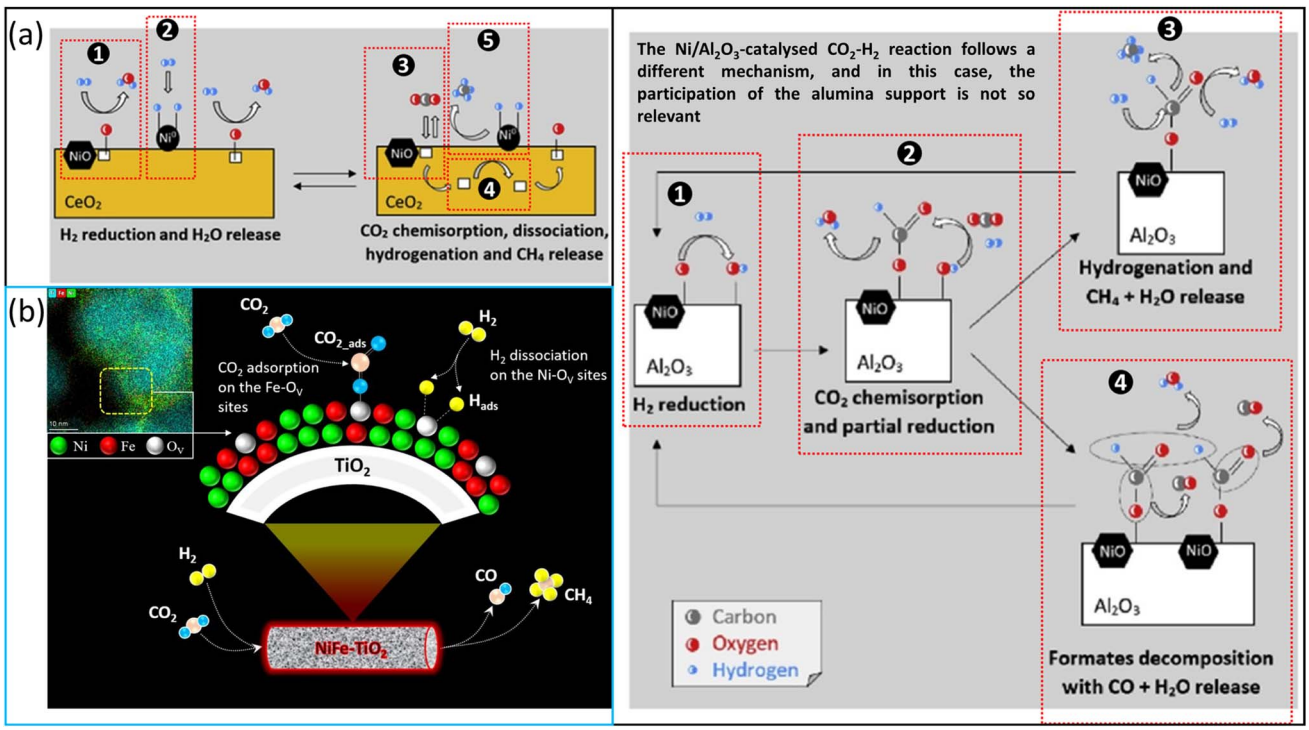

Fig. 14 The CO_2 methanation reaction pathways on (a) CeO_2 and Al_2O_3 support (this figure has been reproduced from ref. 112 with permission from Elsevier, copyright 2020). (b) The schematic representation of NiFe–TiO_2 catalyst (this figure has been reproduced from ref. 14 with permission from Elsevier, copyright 2024).

5. *In situ* characterization techniques for unveiling the CO_2 methanation reaction pathway

In situ characterization techniques play a pivotal role in uncovering the intricate reaction mechanisms of CO_2 methanation, providing real-time insights into the dynamic changes occurring on catalyst surfaces under reaction conditions. Advanced methods such as *in situ* X-ray absorption spectroscopy (XAS) and ambient-pressure X-ray photoelectron spectroscopy (AP-XPS) enable the investigation of oxidation states and electronic structures of active sites. Additionally, techniques like diffuse reflectance infrared Fourier transform spectroscopy (DRIFTS) allow the identification of surface-adsorbed intermediates, revealing the sequential steps of CO_2 activation and hydrogenation. Combining these tools with *operando* setups further bridges the gap between experimental observations and catalytic performance, offering a comprehensive understanding of reaction pathways. This detailed knowledge is instrumental for rational catalyst design, enabling the optimization of activity, selectivity, and durability for efficient CO_2 conversion. The more details about aforementioned technologies are given in following section.

5.1. *In situ* X-ray absorption spectroscopy (XAS)

In situ XAS is a powerful tool for investigating the dynamic structural and electronic changes occurring in catalysts during CO_2 methanation. By providing element-specific insights into oxidation states, local atomic environments, and coordination changes under reaction conditions, *in situ* XAS enables a deeper understanding of the active sites and reaction intermediates.[14] For instance, it can reveal the role of reducible metal oxides or metal–support interactions by tracking the evolution of oxidation states and structural transformations in real-time. This information is crucial for elucidating reaction mechanisms, identifying active phases, and optimizing catalyst design to enhance performance and durability in CO_2 methanation. Beniwal *et al.* used *in situ* XAS analysis to reveal the potential synergy between oxygen vacancies, Ni and Fe sites during CO_2 methanation.[14] Insights gained from *in situ* XAS and ambient pressure X-ray photoelectron spectroscopy revealed critical performance descriptors and reaction pathways. These studies highlighted the synergistic role of oxygen vacancies within atomic Fe-oxide clusters and adjacent Ni-hydroxide domains in facilitating both CO_2 activation and H_2 dissociation. This synergy effectively supports the seamless progression of intermediate steps, significantly enhancing the kinetics of CO_2 methanation on the NiFe–TiO_2 catalyst surface.

5.2. Ambient pressure X-ray photoelectron spectroscopy (APXPS)

The APXPS is a powerful tool for probing surface chemistry and reaction mechanisms during CO_2 methanation under near-operational conditions. It provides real-time insights into the electronic states and chemical interactions at the catalyst surface, enabling the identification of key intermediates and reaction pathways. APXPS helps elucidate how active sites, such as metal–support interfaces or oxygen vacancies, facilitate CO_2 activation and hydrogen dissociation. By tracking surface species and their evolution, this technique offers valuable information for optimizing catalyst design and improving overall methanation efficiency. For instance, Yan *et al.* used APXPS analysis to reveal the synergistic collaboration between adjacent reaction sites of Ni and Pd for CO_2 methanation.[113] A hierarchically structured bimetallic nanocatalyst (NC), designated as NiOTPd-T, has been developed through a methodical process involving sequential metal ion adsorption followed by wet chemical reduction on a carbon nanotube support. This nanocatalyst features metallic Pd nanoclusters in proximity to locally tetrahedral symmetric Ni-oxide and is further modified with a thin tetramethyl orthosilicate (TMOS) layer. Utilizing a combination of structural characterization techniques, *in situ* ambient pressure X-ray photoelectron spectroscopy, and gas chromatography-mass spectrometry, the NiOTPd-T catalyst demonstrated a remarkable methane production yield of 1905.1 mmol g^{-1} at 573 K, exceeding TMOS-decorated Pd-only catalysts (Pd-T) by over tenfold. This exceptional performance is attributed to the synergistic interaction between CO adsorption on Pd atoms and hydrogen dissociation on both Pd and Ni atoms at the interface. This collaboration activates a chain of reactions where the reduction of NiOT increases metallic Ni sites, further enhancing hydrogen splitting and optimizing methane production. Notably, the unique epitaxial arrangement of Pd and NiOT in the NiOTPd-T catalyst delivers an unparalleled methane production yield among comparable catalysts with similar compositions and loadings, making it a benchmark for catalytic efficiency in this domain. Furthermore, in another study, they revealed the interplay between oxygen vacancies and surface silicide using APXPS for enhanced CO_2 methanation.[20]

5.3. *In situ* diffuse reflectance infrared Fourier transform spectroscopy (DRIFTS)

The *in situ* DRIFTS plays a crucial role in studying CO_2 methanation by providing real-time insights into surface species and reaction intermediates.[112] By directly monitoring the catalyst surface during reaction, DRIFTS allows for the identification and characterization of key reaction intermediates, such as formates or carbonates, and the evolution of surface-bound species. This enhances the understanding of the reaction mechanism, facilitates the optimization of catalyst properties, and helps in improving the efficiency of CO_2 conversion to methane. The ability to perform *in situ* measurements under reaction conditions ensures more accurate, dynamic data compared to *ex situ* techniques, providing valuable information for catalyst design and process development.

5.4. *In situ* Raman spectroscopy

In situ Raman spectroscopy offers unique insights into the molecular transformations occurring on the catalyst surface during reaction conditions, providing real-time, non-

destructive analysis. The process involves the interaction of CO_2 with H_2 over a catalyst surface, typically transition metals or metal oxides, under controlled temperature and pressure conditions. Raman spectroscopy, through its ability to probe vibrational modes of molecules and surface intermediates, enables the identification of active sites, reaction intermediates, and the determination of reaction pathways. CO_2 methanation *via in situ* Raman spectroscopy involves several key steps and considerations.[114] Firstly, during the initial adsorption of CO_2 and H_2 on the catalyst surface, Raman spectra can reveal changes in vibrational frequencies that indicate the formation of adsorbed species such as CO_2^*, CO*, and H*. These species act as precursors to subsequent reaction steps. As the reaction progresses, monitoring changes in these vibrational modes can elucidate the kinetics of surface reactions, including the formation of CH_4 and water. Moreover, *in situ* Raman spectroscopy provides invaluable information on catalyst stability and deactivation mechanisms. By continuously monitoring changes in spectra during prolonged reaction times, researchers can identify catalyst poisoning or structural changes that lead to reduced activity or selectivity. This capability is critical for designing more robust and efficient catalyst materials for CO_2 methanation processes. Several studies have utilized *in situ* Raman spectroscopy to investigate CO_2 methanation on various catalyst systems. For example, research by Mutz *et al.* demonstrated the use of *in situ* Raman spectroscopy to track the formation of CH_4 and CO intermediates on Ni-based catalysts.[115] The study highlighted the role of surface morphology and metal–support interactions in influencing catalytic performance. Similarly, work by Gao *et al.* employed Raman spectroscopy to study the role of surface defects on ruthenium-based catalysts in the CO_2 methanation.[116] In summary, *in situ* Raman spectroscopy serves as a powerful tool for advancing our understanding of CO_2 methanation processes by providing detailed molecular-level insights into catalyst behavior, reaction mechanisms, and kinetics. Its ability to monitor surface species and reaction intermediates in real time contributes significantly to the development of efficient catalysts for sustainable CO_2 conversion technologies. Future research directions may focus on further enhancing the sensitivity and spatial resolution of Raman spectroscopy techniques to explore complex catalyst systems and optimize process parameters for enhanced CO_2 utilization and methane production.

6. Photocatalytic CO_2 methanation: a sustainable alternative to thermal CO_2 methanation

6.1. Introduction

The conversion of CO_2 into CH_4 is a promising approach to mitigating greenhouse gas emissions and producing a renewable energy carrier. While thermal CO_2 methanation, commonly known as the Sabatier reaction, has been widely studied and industrially implemented, its reliance on high temperatures (200–500 °C) imposes significant energy and economic costs. In contrast, photocatalytic CO_2 methanation offers a sustainable alternative by utilizing solar energy to drive the reaction under mild conditions, reducing the dependency on fossil fuel-derived heat sources.[117–125] This section explores the mechanisms, catalysts, and recent advancements in photocatalytic CO_2 methanation and how it compares with its thermal counterpart.

6.2. Comparison between thermal and photocatalytic CO_2 methanation

Thermal CO_2 methanation, which was discussed in the previous section, typically employs transition-metal-based catalysts such as nickel (Ni), or cobalt (Co) supported on oxides (*e.g.*, Al_2O_3, TiO_2, CeO_2).[126–131] These catalysts facilitate CO_2 activation and hydrogenation to methane *via* a surface-mediated reaction mechanism. *In situ* Raman spectroscopy has proven to be an essential tool in studying reaction intermediates, active sites, and catalyst stability under thermal conditions. In contrast, photocatalytic CO_2 methanation relies on the absorption of solar photons to generate electron–hole pairs in semiconductor catalysts, which subsequently drive CO_2 reduction and H_2 oxidation reactions. This process occurs at ambient temperatures and pressures, making it a greener and more energy-efficient alternative. However, the reaction efficiency and selectivity are often limited by issues such as low photon absorption, fast charge recombination, and insufficient catalyst stability.

6.3. Mechanism of photocatalytic CO_2 methanation

The mechanism of photocatalytic CO_2 methanation can be divided into the following key steps:

(1) Photon absorption: a semiconductor photocatalyst absorbs light with energy equal to or greater than its bandgap, generating excited electron–hole pairs.

(2) Charge separation and transfer: the photoexcited electrons migrate to the conduction band while the holes remain in the valence band. Effective charge separation is crucial for preventing recombination, which reduces photocatalytic efficiency.

(3) Surface reactions: the excited electrons reduce CO_2 adsorbed on the catalyst surface through intermediate species such as CO_2^-, CO, and $HCOO^-$. Simultaneously, hydrogen oxidation or water splitting occurs *via* hole-mediated reactions.

(4) Methane formation: successive proton-coupled electron transfer steps lead to the formation of CH_4 as the final product, along with possible by-products such as CO and H_2.

6.4. Catalyst development for photocatalytic CO_2 methanation

The choice of photocatalyst is critical for achieving high activity and selectivity in CO_2 methanation. Some of the most studied photocatalysts include:

6.4.1. TiO_2-based photocatalysts. Titanium dioxide (TiO_2) is one of the most widely explored photocatalysts due to its stability, non-toxicity, and abundance. However, its wide bandgap (~3.2 eV) limits its absorption to the UV region (~5%

of the solar spectrum). To enhance its performance, researchers have employed strategies such as:

(i) Doping with metals (*e.g.*, Ni, Cu, or Ru) and non-metals (*e.g.*, N, C, S) to extend light absorption into the visible region.

(ii) Coupling with plasmonic nanoparticles (*e.g.*, Au, Ag) to improve charge transfer and enhance localized surface plasmon resonance (LSPR).

(iii) Surface modification with oxygen vacancies and co-catalysts (*e.g.*, Pt, Ru) to enhance CO_2 activation.

6.4.2. Perovskite photocatalysts. Perovskite materials such as $LaCoO_3$ and $SrTiO_3$ have gained attention due to their tunable electronic properties and excellent charge transport characteristics. These materials exhibit strong visible light absorption and can be further optimized by:

(i) Substituting A- or B-site cations (*e.g.*, La → Ce, Co → Ni) to modulate electronic structure.

(ii) Incorporating heterojunctions with TiO_2 or g-C_3N_4 to enhance charge separation.

6.4.3. Metal–organic frameworks (MOFs) and covalent organic frameworks (COFs). MOFs and CFs are emerging photocatalysts due to their high surface area, tunable porosity, and ability to anchor active metal sites. For example, Ru-based MOFs have shown high selectivity for methane formation under visible light irradiation. However, their stability remains a challenge, necessitating the development of hybrid structures with stable inorganic supports.

6.4.4. Graphitic carbon nitride (g-C_3N_4). Graphitic carbon nitride (g-C_3N_4) has attracted interest due to its narrow bandgap (~2.7 eV), allowing visible light absorption. It can be further modified through:

(i) Heterojunction formation with other semiconductors like TiO_2, ZnO, and MoS_2.

(ii) Doping with heteroatoms such as boron (B) or phosphorus (P) to enhance conductivity.

(iii) Loading with transition metal nanoparticles (*e.g.*, Ni, Ru) to improve catalytic activity.

6.5. Challenges and future perspectives

Despite the potential of photocatalytic CO_2 methanation, several challenges hinder its widespread implementation:[132]

(i) Low quantum efficiency: due to rapid charge recombination and limited light absorption, photocatalytic efficiency remains lower than thermal processes.

(ii) Selectivity issues: competing side reactions such as CO_2-to-CO reduction or H_2 evolution can reduce methane selectivity.

(iii) Long-term stability: many photocatalysts suffer from degradation over time, necessitating durable materials with strong resistance to photodegradation.

(iv) Scale-up and integration: industrial-scale implementation requires efficient light management strategies, reactor design optimization, and integration with renewable hydrogen production.

To address these issues, future research should focus on:

(i) Developing multi-component heterojunctions to facilitate charge separation.

(ii) Engineering catalysts with controlled defect structures for enhanced CO_2 adsorption.

(iii) Designing photoreactors that optimize photon utilization and heat management.

(iv) Integrating photocatalytic methanation with electrochemical and bio-catalytic approaches for hybrid CO_2 conversion systems.

In summary, photocatalytic CO_2 methanation presents a promising alternative to conventional thermal CO_2 methanation by leveraging solar energy to drive the reaction under ambient conditions. While thermal CO_2 methanation remains the most industrially viable process due to its high efficiency and well-established technology, advancements in photocatalyst design and light-harvesting strategies are steadily improving the feasibility of photocatalytic routes. Bridging the gap between these two approaches through hybrid thermal-photocatalytic systems could offer a pathway toward scalable and sustainable CO_2-to-CH_4 conversion technologies. Continued research into material innovation, reaction engineering, and process integration will be essential for realizing the full potential of photocatalytic CO_2 methanation in future energy and carbon management systems.

7. Density functional theory (DFT) approach for designing high-performance CO_2 thermal and photocatalysts

The development of efficient catalysts for CO_2 conversion, whether through thermal or photocatalytic pathways, requires a fundamental understanding of reaction mechanisms, active sites, and electronic structures. Density Functional Theory (DFT) has emerged as a powerful computational tool for designing and optimizing catalysts by providing atomistic insights into catalytic activity, stability, and selectivity.[133] By modelling the electronic structure of materials and their interactions with CO_2 and reaction intermediates, DFT enables researchers to tailor catalyst compositions and structures for enhanced performance.[134] This section discusses the role of DFT in designing high-performance CO_2 methanation catalysts, bridging thermal and photocatalytic processes.

7.1. DFT in thermal CO_2 methanation catalyst design

Thermal CO_2 methanation, often facilitated by transition metal catalysts such as Ni, Ru, and Co, involves multiple adsorption, dissociation, and hydrogenation steps. DFT plays a crucial role in predicting:

(1) Catalyst surface reactivity: by calculating adsorption energies of CO_2 and intermediates (CO, $HCOO^-$, CH_3O^-), DFT helps identify the most active surface facets and sites for CO_2 conversion.

(2) Activation energy and reaction pathways: transition state analysis allows the estimation of energy barriers for key reaction steps, guiding catalyst modification to lower activation energies.

(3) Metal–support interactions: DFT studies on metal-oxide interfaces (*e.g.*, Ni/CeO_2, Ru/TiO_2) reveal charge transfer mechanisms and oxygen vacancy roles in enhancing catalytic activity.

(4) Poisoning and stability: computational modeling of sulfur, carbon, and oxygen interactions on catalyst surfaces aids in designing more resistant and durable catalysts.

7.2. DFT in photocatalytic CO_2 methanation

For photocatalytic CO_2 methanation, DFT is instrumental in designing semiconductor-based catalysts by optimizing their electronic structures for efficient light absorption and charge separation. Key contributions of DFT include:

(1) Band structure engineering: DFT helps in calculating bandgap energies and band edge positions, ensuring suitable alignment for CO_2 reduction and H_2 oxidation.

(2) Defect engineering: the role of surface defects, oxygen vacancies, and dopants in modifying charge carrier dynamics and adsorption properties can be systematically studied using DFT.

(3) Heterojunction design: interface modeling between semiconductors (*e.g.*, TiO_2/g-C_3N_4, ZnO/MoS_2) predicts charge transfer efficiency, guiding the selection of materials for enhanced photocatalytic activity.

(4) Surface adsorption and reaction kinetics: by determining adsorption energies and reaction pathways of CO_2-derived intermediates, DFT provides insights into selectivity control and product formation mechanisms.

The integration of DFT with experimental studies, machine learning, and *in situ* spectroscopy will further accelerate the discovery of novel CO_2 methanation catalysts. Advanced simulations incorporating solvation effects, dynamic charge redistribution, and large-scale reaction networks will improve the predictive power of DFT. Hybrid computational approaches combining DFT with microkinetic modeling can offer more accurate insights into real-world catalytic performance, paving the way for next-generation high-efficiency catalysts. DFT-based computational modeling has revolutionized catalyst design for CO_2 methanation by offering atomic-level insights into reaction mechanisms and material properties. Its application in both thermal and photocatalytic systems enables the development of tailored catalysts with improved activity, stability, and selectivity. As computational power and algorithms continue to evolve, DFT-driven catalyst design will play an increasingly vital role in advancing CO_2 conversion technologies toward sustainable energy solutions.

8. Industrial applications of CO_2 methanation

CO_2 methanation has gained significant industrial interest as a key process for carbon capture and utilization (CCU), energy storage, and synthetic fuel production.[135] One of the most promising applications is power-to-gas technology, where surplus renewable electricity is used to produce hydrogen *via* water electrolysis, which is then combined with captured CO_2 to generate methane.[136] This methane, also known as synthetic natural gas (SNG), can be directly injected into existing natural gas grids, providing a scalable solution for long-term energy storage and grid balancing. Several industrial-scale PtG plants have been established in Europe, such as Audi's e-gas facility in Germany, which produces renewable methane for transportation applications.

Another critical application of CO_2 methanation is in biogas upgrading, where CO_2 present in raw biogas is converted into methane, increasing its calorific value and making it compatible with natural gas infrastructure.[137] This approach enhances the efficiency of biogas utilization by maximizing methane yield while simultaneously reducing greenhouse gas emissions. Industrial biogas upgrading systems employing catalytic methanation have been developed to produce high-purity biomethane, which can be used as a sustainable fuel for power generation and transportation. CO_2 methanation also plays a vital role in closed-loop carbon recycling for space and aerospace applications. For instance, the Sabatier process is integrated into the International Space Station (ISS) to convert astronaut-exhaled CO_2 into methane and water, with the latter being recycled for life-support systems. This concept is being explored for future Mars missions, where *in situ* resource utilization (ISRU) could enable methane production for rocket fuel using Martian CO_2 and hydrogen from water electrolysis. Additionally, methane production *via* CO_2 methanation is gaining traction in industrial sectors looking to decarbonize operations, particularly in steel, cement, and chemical manufacturing. By capturing CO_2 emissions from these industries and converting them into methane, companies can create a circular carbon economy while reducing reliance on fossil fuels. Furthermore, the synthesized methane can be utilized as a feedstock for further chemical synthesis, including the production of methanol and higher hydrocarbons *via* Fischer–Tropsch processes. In summary, CO_2 methanation is emerging as a pivotal technology in multiple industrial sectors, enabling sustainable energy storage, low-carbon fuel production, and carbon recycling. Continued advancements in catalyst development, reactor design, and integration with renewable energy sources will further enhance its commercial viability and environmental benefits.

9. Summary and outlook

The increasing concentration of CO_2 in the atmosphere and its role as a primary driver of climate change have underscored the urgent need for technologies that enable efficient CO_2 conversion and utilization. Among these, CO_2 methanation offers a promising route to produce methane, a clean and energy-dense fuel, while simultaneously reducing atmospheric CO_2 levels. Over the past decades, significant advancements have been made in designing catalysts to enhance the efficiency, selectivity, and stability of the CO_2 methanation process. Key developments in catalyst design strategies have revolved around optimizing active metal components, supports, and promoter elements to achieve superior catalytic performance. Nickel-based catalysts, owing to their cost-effectiveness and high activity, have been widely explored. The incorporation of

secondary metals, such as cobalt, iron, and noble metals (*e.g.*, Ru, Rh, Pd), has led to the development of bimetallic and multimetallic catalysts that exhibit synergistic effects, including enhanced reducibility, better dispersion, and improved resistance to deactivation. The role of support materials, such as CeO_2, Al_2O_3, TiO_2, ZrO_2, and SiO_2, has also been extensively studied. Supports contribute significantly to catalytic activity by influencing metal dispersion, providing structural stability, and facilitating the adsorption and activation of CO_2 and H_2. Reducible oxides like CeO_2 and ZrO_2 have garnered particular attention due to their ability to generate oxygen vacancies, which act as active sites for CO_2 activation and intermediate stabilization. Furthermore, the interaction between active metals and support materials plays a crucial role in determining catalytic performance, as demonstrated in Ni/CeO_2 and Ni/Al_2O_3 systems. Promoters, such as alkali and alkaline earth metals, have been employed to fine-tune catalyst properties. These promoters enhance CO_2 adsorption, alter electronic properties, and improve the reducibility of active metal species, leading to better catalytic efficiency. For example, the addition of potassium and magnesium has been shown to boost CO_2 adsorption while suppressing undesirable side reactions. The development of novel synthesis techniques has further refined catalyst design. Methods such as co-precipitation, sol–gel synthesis, impregnation, and chemical vapor deposition have been utilized to control the morphology, particle size, and distribution of active metal species. Advanced strategies like the use of ordered mesoporous supports, core–shell structures, and atomically dispersed catalysts have yielded materials with enhanced catalytic activity, stability, and resistance to sintering and coking. Mechanistic insights gained through advanced characterization techniques, including *in situ* X-ray absorption spectroscopy (XAS), ambient pressure X-ray photoelectron spectroscopy (AP-XPS), and transmission electron microscopy (TEM), have deepened our understanding of the CO_2 methanation process. These studies have elucidated reaction pathways, identified key intermediates, and highlighted the importance of oxygen vacancies, metal–support interactions, and the role of formate and carbonate species in the reaction mechanism. Despite these advancements, several challenges remain. Catalyst deactivation due to sintering, carbon deposition, and sulfur poisoning poses significant barriers to long-term operation. Additionally, the optimization of reaction conditions, such as temperature, pressure, and H_2/CO_2 ratios, is crucial to maximize methane selectivity and yield.

The future of catalyst design for CO_2 methanation lies in addressing current challenges and leveraging emerging technologies to develop robust, efficient, and scalable catalytic systems. Below are key areas for future research and development:

(1) Advanced catalyst architectures:

○ The design of catalysts with hierarchical structures, such as core–shell and yolk–shell architectures, can enhance active site accessibility and prevent sintering and coking.

○ The use of atomically dispersed catalysts and single-atom alloys offers potential for achieving maximum atom efficiency and exceptional catalytic performance.

(2) Exploration of novel materials:

○ Beyond traditional supports, the exploration of materials such as metal–organic frameworks (MOFs), covalent organic frameworks (COFs), and hybrid systems can open new avenues for catalyst development.

○ Transition metal carbides and nitrides, with their unique electronic properties, represent promising alternatives to conventional catalysts.

(3) Tailored oxygen vacancy engineering:

○ Precise control over oxygen vacancy generation in reducible supports like CeO_2 and ZrO_2 can further enhance CO_2 activation and intermediate stabilization.

○ Strategies to stabilize oxygen vacancies under reaction conditions will be crucial for long-term catalyst durability.

(4) Integration of computational and experimental approaches:

○ The use of density functional theory (DFT) calculations and machine learning algorithms can accelerate the discovery of new catalyst compositions and optimize reaction conditions.

○ High-throughput screening techniques can complement computational studies, enabling rapid identification of promising candidates.

(5) Improved resistance to deactivation:

○ Developing catalysts with enhanced resistance to sintering, coking, and poisoning by sulfur and other impurities will be vital for industrial applications.

○ Coating active sites with protective layers or incorporating self-regenerative mechanisms can prolong catalyst lifespan.

(6) Mechanistic understanding and *operando* studies:

○ Advanced *in situ* and *operando* characterization techniques will continue to play a pivotal role in unraveling reaction mechanisms and identifying active sites.

○ The development of techniques that allow real-time monitoring of catalytic processes under industrially relevant conditions will bridge the gap between fundamental research and practical applications.

(7) Energy efficiency and sustainability:

○ Coupling CO_2 methanation with renewable hydrogen production (*e.g.*, *via* water electrolysis powered by solar or wind energy) will enhance the sustainability of the process.

○ Exploring catalysts that operate efficiently at lower temperatures and pressures can reduce energy consumption and operational costs.

(8) Scale-up and industrial implementation:

○ Translating laboratory-scale findings to industrial-scale processes requires the development of robust catalysts that maintain performance under high space velocities and prolonged operation.

○ Collaboration between academia, industry, and policymakers will be essential to overcome barriers to commercialization.

(9) Integration into carbon utilization pathways:

○ CO_2 methanation can be integrated into broader carbon utilization frameworks, such as synthetic natural gas (SNG) production, power-to-gas technologies, and carbon capture and utilization (CCU) systems.

○ Developing multi-functional catalysts capable of co-converting CO_2 with other waste streams (*e.g.*, CO, syngas, or biomass-derived intermediates) can enhance process versatility.

(10) Environmental and economic assessment:

○ Life cycle assessment (LCA) and techno-economic analysis (TEA) will be crucial for evaluating the environmental and economic viability of CO_2 methanation technologies.

○ Identifying cost-effective and scalable synthesis methods for catalyst production will be key to enabling widespread adoption.

10. Conclusion

Catalyst design strategies for CO_2 methanation have made significant strides in recent years, offering promising solutions for both CO_2 utilization and methane production. CO_2 methanation, the process of converting carbon dioxide into methane (CH_4) through a reaction with hydrogen (H_2), is a key component in the broader quest for carbon-neutral energy solutions. Methane, as a natural gas, is an energy carrier with a relatively high energy density and can be used in a variety of applications, including power generation, transportation, and heating. However, the transition to a more sustainable energy system requires the efficient and scalable conversion of CO_2 into methane, and this depends largely on the development of advanced catalysts. Over the years, catalytic systems have evolved to improve both activity and selectivity in CO_2 methanation. Early catalysts, such as nickel-based and cobalt-based systems, were widely studied due to their low cost and relatively good performance. However, these catalysts often suffer from limitations such as deactivation over time, low resistance to sintering, and reduced efficiency under reaction conditions. Newer approaches have focused on improving catalyst stability, enhancing CO_2 adsorption properties, and fine-tuning the reaction mechanism to reduce side reactions like reverse water–gas shift (RWGS), which produces CO and limits the overall methane yield. One of the most promising strategies for next-generation catalyst development is the incorporation of bimetallic and alloy catalysts. These catalysts, which typically involve a combination of metals like nickel with transition metals such as copper, palladium, or platinum, offer enhanced performance by providing synergistic effects that improve the activation of CO_2 and H_2. By fine-tuning the electronic and geometric properties of the metal surfaces, these bimetallic systems can achieve higher CO_2 conversion rates while maintaining long-term stability. Additionally, advances in nanostructuring, such as the creation of smaller particle sizes or the development of core–shell structures, help maximize surface area and increase catalytic activity. Another exciting avenue for catalyst design lies in the use of metal–organic frameworks (MOFs) and other porous materials. These materials can be engineered to provide a high surface area for CO_2 adsorption and activation, making them excellent candidates for catalysis. MOFs, in particular, offer a high degree of tunability, with specific pore sizes and functional groups that can be tailored for optimal CO_2 interaction. *In situ* techniques such as Diffuse Reflectance Infrared Fourier Transform Spectroscopy (DRIFTS) are critical in understanding how these catalysts interact with CO_2 and H_2 at the atomic level, helping to refine their performance and ensure more efficient reactions. Furthermore, interdisciplinary approaches combining catalysis with advances in renewable energy and carbon capture technologies are helping to accelerate the development of CO_2 methanation as a commercially viable process. For example, integrating CO_2 methanation with renewable energy sources like solar, wind, or biomass-derived hydrogen creates a sustainable cycle in which excess renewable energy can be stored in the form of methane. This creates an effective energy storage solution, addressing the intermittency issues associated with renewable energy sources. Additionally, coupling CO_2 methanation with carbon capture systems allows for the direct utilization of CO_2 from industrial emissions, helping mitigate climate change by reducing atmospheric CO_2 concentrations. The integration of these advancements holds immense potential to transform CO_2 methanation into a cornerstone technology for a sustainable and circular carbon economy. With further research and innovation, these technologies could significantly reduce greenhouse gas emissions and provide a scalable pathway for mitigating climate change. The development of efficient and robust catalysts will enable the conversion of waste CO_2 into a valuable energy resource, contributing to a circular carbon economy where carbon is continuously recycled and utilized rather than emitted into the atmosphere. In conclusion, the continuous advancements in catalyst design, coupled with innovative interdisciplinary approaches, are creating a new era for CO_2 methanation. The synergy between CO_2 conversion, renewable energy, and carbon capture technologies will not only drive the development of more efficient and sustainable catalysts but also pave the way for a greener, more sustainable future where CO_2 can be captured, converted, and reused as a valuable resource. The path forward promises a significant step toward achieving a sustainable, low-carbon economy and addressing global climate challenges.

Data availability

No new data were generated or analysed as part of this review.

Conflicts of interest

The authors declare no conflict of interest.

Acknowledgements

Dinesh Bhalothia acknowledges the funding support from Manipal University Jaipur (Enhanced Seed Grant EF/2024-25/QE-04-08). Ashima Bagaria acknowledges the funding support from the Department of Science and Technology, Rajasthan, India. Project Ref: (P.7(3) DST/BTR & D/EAC/2018/3146-56). T.-Y. Chen acknowledges the funding support from the National Science and Technology Council, Taiwan (NSTC 112-2112-M-007-026-) and the industrial collaboration projects from the MA-tek (MA-tek 2023-T-004) and the Taiwan Space Agency (TASA-S-1120691).

References

1 K. O. Yoro and M. O. Daramola, in *Advances in Carbon Capture*, ed. M. R. Rahimpour, M. Farsi and M. A. Makarem, Woodhead Publishing, 2020, pp. 3–28, DOI: 10.1016/B978-0-12-819657-1.00001-3.
2 M. Amin, H. H. Shah, A. G. Fareed, W. U. Khan, E. Chung, A. Zia, Z. U. Rahman Farooqi and C. Lee, *Int. J. Hydrogen Energy*, 2022, **47**, 33112–33134.
3 D. Bhalothia, W.-H. Hsiung, S.-S. Yang, C. Yan, P.-C. Chen, T.-H. Lin, S.-C. Wu, P.-C. Chen, K.-W. Wang, M.-W. Lin and T.-Y. Chen, *ACS Appl. Energy Mater.*, 2021, **4**, 14043–14058.
4 J. A. Cruz-Navarro, F. Hernández-García, A. T. Sánchez-Mora, M. E. Moreno-Narváez, V. Reyes-Márquez, R. Colorado-Peralta and D. Morales-Morales, *Methane*, 2024, **3**, 466–484.
5 J. Ashok, S. Pati, P. Hongmanorom, Z. Tianxi, C. Junmei and S. Kawi, *Catal. Today*, 2020, **356**, 471–489.
6 C. Mebrahtu, F. Krebs, S. Abate, S. Perathoner, G. Centi and R. Palkovits, in *Studies in Surface Science and Catalysis*, ed. S. Albonetti, S. Perathoner and E. A. Quadrelli, Elsevier, 2019, vol. 178, pp. 85–103.
7 J. Ma, N. Sun, X. Zhang, N. Zhao, F. Xiao, W. Wei and Y. Sun, *Catal. Today*, 2009, **148**, 221–231.
8 P. K. Saravanan, D. Bhalothia, A. Beniwal, C.-H. Tsai, P.-Y. Liu, T.-Y. Chen, H.-M. Ku and P.-C. Chen, *Catalysts*, 2024, **14**(7), 410.
9 M. Younas, L. Loong Kong, M. J. K. Bashir, H. Nadeem, A. Shehzad and S. Sethupathi, *Energy Fuels*, 2016, **30**, 8815–8831.
10 E. Baraj, S. Vagaský, T. Hlinčik, K. Ciahotný and V. Tekáč, *Chem. Pap.*, 2016, **70**, 395–403.
11 D. Bhalothia, A. Beniwal, P. Kumar Saravanan, P.-C. Chen and T.-Y. Chen, *ChemElectroChem*, 2024, **11**, e202400034.
12 W. N. R. W. Isahak and A. Al-Amiery, *Green Technol. Sustainability*, 2024, **2**, 100078.
13 R. Singh, L. Wang and J. Huang, *ChemPlusChem*, 2024, **89**, e202300511.
14 A. Beniwal, D. Bhalothia, Y.-R. Chen, J.-C. Kao, C. Yan, N. Hiraoka, H. Ishii, M. Cheng, Y.-C. Lo, X. Tu, Y.-W. Chiang, C.-H. Kuo, J.-P. Chou, C.-H. Wang and T.-Y. Chen, *Chem. Eng. J.*, 2024, **493**, 152834.
15 J. Ren, H. Guo, J. Yang, Z. Qin, J. Lin and Z. Li, *Appl. Surf. Sci.*, 2015, **351**, 504–516.
16 Q. Pan, J. Peng, T. Sun, S. Wang and S. Wang, *Catal. Commun.*, 2014, **45**, 74–78.
17 J. Kim, Y. Yu, T. W. Go, J.-J. Gallet, F. Bournel, B. S. Mun and J. Y. Park, *Nat. Commun.*, 2023, **14**, 3273.
18 Y. Yang, J. Liu, F. Liu and D. Wu, *Fuel*, 2020, **276**, 118093.
19 I. Hussain, A. A. Jalil, N. S. Hassan and M. Y. S. Hamid, *J. Energy Chem.*, 2021, **62**, 377–407.
20 T. Yang, A. Beniwal, D. Bhalothia, C. Yan, C.-H. Wang and T.-Y. Chen, *Sustainable Energy Fuels*, 2024, **8**, 3399–3411.
21 P. Strucks, L. Failing and S. Kaluza, *Chem. Ing. Tech.*, 2021, **93**, 1526–1536.
22 S. Sikiru, T. L. Oladosu, T. I. Amosa, J. O. Olutoki, M. N. M. Ansari, K. J. Abioye, Z. U. Rehman and H. Soleimani, *Int. J. Hydrogen Energy*, 2024, **56**, 1152–1182.
23 Z. Uddin, B.-Y. Yu and H.-Y. Lee, *J. CO_2 Util.*, 2022, **60**, 101974.
24 W. K. Fan and M. Tahir, *J. Environ. Chem. Eng.*, 2021, **9**, 105460.
25 G. Varvoutis, M. Lykaki, G. E. Marnellos and M. Konsolakis, *Catalysts*, 2023, **13**(2), 275.
26 L. Xu, Y. Cui, M. Chen, X. Wen, C. Lv, X. Wu, C.-e. Wu, Z. Miao and X. Hu, *Ind. Eng. Chem. Res.*, 2021, **60**, 8056–8072.
27 A. Erdőhelyi, *Catalysts*, 2021, 11.
28 H. Kang, L. Zhu, S. Li, S. Yu, Y. Niu, B. Zhang, W. Chu, X. Liu, S. Perathoner, G. Centi and Y. Liu, *Nat. Catal.*, 2023, **6**, 1062–1072.
29 J. K. Prabhakar, R. Kumar, K. Ray, P. A. Apte and G. Deo, *J. Environ. Chem. Eng.*, 2025, **13**, 115233.
30 E. Meloni, L. Cafiero, S. Renda, M. Martino, M. Pierro and V. Palma, *Catalysts*, 2023, **13**(3), 488.
31 S. Rönsch, J. Schneider, S. Matthischke, M. Schlüter, M. Götz, J. Lefebvre, P. Prabhakaran and S. Bajohr, *Fuel*, 2016, **166**, 276–296.
32 P. Panagiotopoulou, D. I. Kondarides and X. E. Verykios, *Appl. Catal., A*, 2008, **344**, 45–54.
33 N. D. Mohd Ridzuan, M. S. Shaharun, M. A. Anawar and I. Ud-Din, *Catalysts*, 2022, **12**(5), 469.
34 L. Li, W. Zeng, M. Song, X. Wu, G. Li and C. Hu, *Catalysts*, 2022, **12**(2), 244.
35 J. Liu, C. Li, F. Wang, S. He, H. Chen, Y. Zhao, M. Wei, D. G. Evans and X. Duan, *Catal. Sci. Technol.*, 2013, **3**, 2627–2633.
36 G. Zhi, X. Guo, Y. Wang, G. Jin and X. Guo, *Catal. Commun.*, 2011, **16**, 56–59.
37 S. Tada, T. Shimizu, H. Kameyama, T. Haneda and R. Kikuchi, *Int. J. Hydrogen Energy*, 2012, **37**, 5527–5531.
38 B. Lu and K. Kawamoto, *Fuel*, 2013, **103**, 699–704.
39 S. He, C. Li, H. Chen, D. Su, B. Zhang, X. Cao, B. Wang, M. Wei, D. G. Evans and X. Duan, *Chem. Mater.*, 2013, **25**, 1040–1046.
40 S. Rahmani, M. Rezaei and F. Meshkani, *J. Ind. Eng. Chem.*, 2014, **20**, 1346–1352.
41 I. Graça, L. V. González, M. C. Bacariza, A. Fernandes, C. Henriques, J. M. Lopes and M. F. Ribeiro, *Appl. Catal., B*, 2014, **147**, 101–110.
42 H. Liu, X. Zou, X. Wang, X. Lu and W. Ding, *J. Nat. Gas Chem.*, 2012, **21**, 703–707.
43 E. Jwa, S. B. Lee, H. W. Lee and Y. S. Mok, *Fuel Process. Technol.*, 2013, **108**, 89–93.
44 M. Cai, J. Wen, W. Chu, X. Cheng and Z. Li, *J. Nat. Gas Chem.*, 2011, **20**, 318–324.
45 F. Ocampo, B. Louis, L. Kiwi-Minsker and A.-C. Roger, *Appl. Catal., A*, 2011, **392**, 36–44.
46 J. Kirchner, J. K. Anolleck, H. Lösch and S. Kureti, *Appl. Catal., B*, 2018, **223**, 47–59.

47 S. N. Bukhari, C. C. Chong, H. D. Setiabudi, N. Ainirazali, M. A. A. Aziz, A. A. Jalil and S. Y. Chin, *Int. J. Hydrogen Energy*, 2019, **44**, 7228–7240.
48 L. Lin, C. A. Gerlak, C. Liu, J. Llorca, S. Yao, N. Rui, F. Zhang, Z. Liu, S. Zhang, K. Deng, C. B. Murray, J. A. Rodriguez and S. D. Senanayake, *J. Energy Chem.*, 2021, **61**, 602–611.
49 F. Song, Q. Zhong, Y. Yu, M. Shi, Y. Wu, J. Hu and Y. Song, *Int. J. Hydrogen Energy*, 2017, **42**, 4174–4183.
50 Z. Refaat, M. E. Saied, A. O. A. E. Naga, S. A. Shaban, H. B. Hassan, M. R. Shehata and F. Y. E. Kady, *Sci. Rep.*, 2023, **13**, 4855.
51 R. Daroughegi, F. Meshkani and M. Rezaei, *Int. J. Hydrogen Energy*, 2017, **42**, 15115–15125.
52 S. Valinejad Moghaddam, M. Rezaei, F. Meshkani and R. Daroughegi, *Int. J. Hydrogen Energy*, 2018, **43**, 16522–16533.
53 E. Medina, A. A. Amell, D. López and A. Santamaría, *Renewable Sustainable Energy Rev.*, 2025, **207**, 114926.
54 Y. Yu, Z. Bian, J. Wang, Z. Wang, W. Tan, Q. Zhong and S. Kawi, *Catal. Today*, 2023, **424**, 113345.
55 L. Shen, J. Xu, M. Zhu and Y.-F. Han, *ACS Catal.*, 2020, **10**, 14581–14591.
56 G. Liao, Y. He, H. Wang, B. Fang, N. Tsubaki and C. Li, *Device*, 2023, **1**, 100173.
57 Y. Bae and J. Hong, *Chem. Eng. J.*, 2022, **446**, 136978.
58 T. Bathena, T. Phung, V. Murugesan, K. A. Goulas, A. S. Karakoti and K. Ramasamy, *J. CO_2 Util.*, 2024, **84**, 102848.
59 Y. Yang, K. Chiang and N. Burke, *Catal. Today*, 2011, **178**, 197–205.
60 W. Yang, K. Chang, M. Yang, X. Yan, S. Yang, Y. Liu, G. Wang, F. Xia, H. Wang and Q. Zhang, *Chem. Eng. J.*, 2024, **499**, 156493.
61 A. Kim, C. Sanchez, G. Patriarche, O. Ersen, S. Moldovan, A. Wisnet, C. Sassoye and D. P. Debecker, *Catal. Sci. Technol.*, 2016, **6**, 8117–8128.
62 J. Martínez, E. Hernández, S. Alfaro, R. López Medina, G. Valverde Aguilar, E. Albiter and M. A. Valenzuela, *Catalysts*, 2019, **9**(1), 24.
63 M. Zhu, P. Tian, X. Cao, J. Chen, T. Pu, B. Shi, J. Xu, J. Moon, Z. Wu and Y.-F. Han, *Appl. Catal., B*, 2021, **282**, 119561.
64 J. Y. Ahn, S. W. Chang, S. M. Lee, S. S. Kim, W. J. Chung, J. C. Lee, Y. J. Cho, K. S. Shin, D. H. Moon and D. D. Nguyen, *Fuel*, 2019, **250**, 277–284.
65 X. Jia, X. Zhang, N. Rui, X. Hu and C.-j. Liu, *Appl. Catal., B*, 2019, **244**, 159–169.
66 C. Guo, Y. Wu, H. Qin and J. Zhang, *Fuel Process. Technol.*, 2014, **124**, 61–69.
67 W. Wang, W. Chu, N. Wang, W. Yang and C. Jiang, *Int. J. Hydrogen Energy*, 2016, **41**, 967–975.
68 F. Hu, S. Tong, K. Lu, C.-M. Chen, F.-Y. Su, J. Zhou, Z.-H. Lu, X. Wang, G. Feng and R. Zhang, *J. CO_2 Util.*, 2019, **34**, 676–687.
69 J. F. da Costa-Serra, C. Cerdá-Moreno and A. Chica, *Appl. Sci.*, 2020, **10**(15), 5131.
70 S. Lin, L. Gong, N. Zhao, H. Zhao, F. Zhao, Y. Bai, Z. Li and W. Liu, *Chem. Eng. J.*, 2024, **494**, 152937.
71 J. Zhou, Z. Gao, G. Xiang, T. Zhai, Z. Liu, W. Zhao, X. Liang and L. Wang, *Nat. Commun.*, 2022, **13**, 327.
72 H. Kang, L. Zhu, S. Li, S. Yu, Y. Niu, B. Zhang, W. Chu, X. Liu, S. Perathoner, G. Centi and Y. Liu, *Nat. Catal.*, 2023, **6**, 1062–1072.
73 K. Xu, C. Ma, H. Yan, H. Gu, W.-W. Wang, S.-Q. Li, Q.-L. Meng, W.-P. Shao, G.-H. Ding, F. R. Wang and C.-J. Jia, *Nat. Commun.*, 2022, **13**, 2443.
74 H. Wang, Z. Li, G. Cui and M. Wei, *ACS Appl. Mater. Interfaces*, 2023, **15**, 19021–19031.
75 P. Hongmanorom, J. Ashok, P. Chirawatkul and S. Kawi, *Appl. Catal., B*, 2021, **297**, 120454.
76 S.-H. Kang, J.-H. Ryu, J.-H. Kim, S.-J. Seo, Y.-D. Yoo, P. S. Sai Prasad, H.-J. Lim and C.-D. Byun, *Korean J. Chem. Eng.*, 2011, **28**, 2282–2286.
77 D. Pandey and G. Deo, *J. Mol. Catal. A: Chem.*, 2014, **382**, 23–30.
78 D. Pandey and G. Deo, *J. Ind. Eng. Chem.*, 2016, **33**, 99–107.
79 K. Ray and G. Deo, *Appl. Catal., B*, 2017, **218**, 525–537.
80 B. Shirsath, M. L. Schulte, B. Kreitz, S. Tischer, J.-D. Grunwaldt and O. Deutschmann, *Chem. Eng. J.*, 2023, **469**, 143847.
81 M.-A. Serrer, K. F. Kalz, E. SaraÇi, H. Lichtenberg and J.-D. Grunwaldt, *ChemCatChem*, 2019, **11**, 5018–5021.
82 C. Mebrahtu, F. Krebs, S. Perathoner, S. Abate, G. Centi and R. Palkovits, *Catal. Sci. Technol.*, 2018, **8**, 1016–1027.
83 M. Guo and G. Lu, *React. Kinet., Mech. Catal.*, 2014, **113**, 101–113.
84 L. Xu, X. Lian, M. Chen, Y. Cui, F. Wang, W. Li and B. Huang, *Int. J. Hydrogen Energy*, 2018, **43**, 17172–17184.
85 L. Xu, X. Lian, M. Chen, Y. Cui, F. Wang, W. Li and B. Huang, *Int. J. Hydrogen Energy*, 2018, **43**, 17172–17184.
86 L. Pastor-Pérez, E. L. Saché, C. Jones, S. Gu, H. Arellano-Garcia and T. R. Reina, *Catal. Today*, 2018, **317**, 108–113.
87 A. Mangla, G. Deo and P. A. Apte, *Comput. Mater. Sci.*, 2018, **153**, 449–460.
88 S.-H. Kang, J.-H. Ryu, J.-H. Kim, S.-J. Seo, Y.-D. Yoo, P. S. Sai Prasad, H.-J. Lim and C.-D. Byun, *Korean J. Chem. Eng.*, 2011, **28**, 2282–2286.
89 J. Sehested, K. E. Larsen, A. L. Kustov, A. M. Frey, T. Johannessen, T. Bligaard, M. P. Andersson, J. K. Nørskov and C. H. Christensen, *Top. Catal.*, 2007, **45**, 9–13.
90 D. Pandey and G. Deo, *J. Mol. Catal. A: Chem.*, 2014, **382**, 23–30.
91 B. Mutz, M. Belimov, W. Wang, P. Sprenger, M.-A. Serrer, D. Wang, P. Pfeifer, W. Kleist and J.-D. Grunwaldt, *ACS Catal.*, 2017, **7**, 6802–6814.
92 S. Farsi, W. Olbrich, P. Pfeifer and R. Dittmeyer, *Chem. Eng. J.*, 2020, **388**, 124233.
93 M.-A. Serrer, A. Gaur, J. Jelic, S. Weber, C. Fritsch, A. H. Clark, E. Saraçi, F. Studt and J.-D. Grunwaldt, *Catal. Sci. Technol.*, 2020, **10**, 7542–7554.
94 C. Mebrahtu, S. Perathoner, G. Giorgianni, S. Chen, G. Centi, F. Krebs, R. Palkovits and S. Abate, *Catal. Sci. Technol.*, 2019, **9**, 4023–4035.

95 Z. Li, T. Zhao and L. Zhang, *Appl. Organomet. Chem.*, 2018, **32**, e4328.
96 C. Liang, Z. Ye, D. Dong, S. Zhang, Q. Liu, G. Chen, C. Li, Y. Wang and X. Hu, *Fuel*, 2019, **254**, 115654.
97 R. Daroughegi, F. Meshkani and M. Rezaei, *J. Energy Inst.*, 2020, **93**, 482–495.
98 M. A. A. Aziz, A. A. Jalil, S. Triwahyono and A. Ahmad, *Green Chem.*, 2015, **17**, 2647–2663.
99 J. Ren, X. Qin, J.-Z. Yang, Z.-F. Qin, H.-L. Guo, J.-Y. Lin and Z. Li, *Fuel Process. Technol.*, 2015, **137**, 204–211.
100 B. Yan, B. Zhao, S. Kattel, Q. Wu, S. Yao, D. Su and J. G. Chen, *J. Catal.*, 2019, **374**, 60–71.
101 H. Lu, X. Yang, G. Gao, J. Wang, C. Han, X. Liang, C. Li, Y. Li, W. Zhang and X. Chen, *Fuel*, 2016, **183**, 335–344.
102 Y. Wu, J. Lin, Y. Xu, G. Ma, J. Wang and M. Ding, *ChemCatChem*, 2020, **12**, 3553–3559.
103 B. Zhao, P. Liu, S. Li, H. Shi, X. Jia, Q. Wang, F. Yang, Z. Song, C. Guo, J. Hu, Z. Chen, X. Yan and X. Ma, *Appl. Catal., B*, 2020, **278**, 119307.
104 Q. Liu, B. Bian, J. Fan and J. Yang, *Int. J. Hydrogen Energy*, 2018, **43**, 4893–4901.
105 B. Alrafei, I. Polaert, A. Ledoux and F. Azzolina-Jury, *Catal. Today*, 2020, **346**, 23–33.
106 N. A. A. Fatah, A. A. Jalil, N. F. M. Salleh, M. Y. S. Hamid, Z. H. Hassan and M. G. M. Nawawi, *Int. J. Hydrogen Energy*, 2020, **45**, 18562–18573.
107 R. Razzaq, H. Zhu, L. Jiang, U. Muhammad, C. Li and S. Zhang, *Ind. Eng. Chem. Res.*, 2013, **52**, 2247–2256.
108 H. Zhu, R. Razzaq, C. Li, Y. Muhmmad and S. Zhang, *AIChE J.*, 2013, **59**, 2567–2576.
109 C. Jia, Y. Dai, Y. Yang and J. W. Chew, *Int. J. Hydrogen Energy*, 2019, **44**, 13443–13455.
110 T. Zhang and Q. Liu, *Int. J. Hydrogen Energy*, 2020, **45**, 4417–4426.
111 F. Hu, R. Ye, C. Jin, D. Liu, X. Chen, C. Li, K. H. Lim, G. Song, T. Wang, G. Feng, R. Zhang and S. Kawi, *Appl. Catal., B*, 2022, **317**, 121715.
112 A. Cárdenas-Arenas, A. Quindimil, A. Davó-Quiñonero, E. Bailón-García, D. Lozano-Castelló, U. De-La-Torre, B. Pereda-Ayo, J. A. González-Marcos, J. R. González-Velasco and A. Bueno-López, *Appl. Catal., B*, 2020, **265**, 118538.
113 C. Yan, C.-H. Wang, M. Lin, D. Bhalothia, S.-S. Yang, G.-J. Fan, J.-L. Wang, T.-S. Chan, Y.-l. Wang, X. Tu, S. Dai, K.-W. Wang, J.-H. He and T.-Y. Chen, *J. Mater. Chem. A*, 2020, **8**, 12744–12756.
114 L. M. Martínez Tejada, A. Muñoz, M. A. Centeno and J. A. Odriozola, *J. Raman Spectrosc.*, 2016, **47**, 189–197.
115 B. Mutz, P. Sprenger, W. Wang, D. Wang, W. Kleist and J.-D. Grunwaldt, *Appl. Catal., A*, 2018, **556**, 160–171.
116 Z. Gao, L. Yang, G. Fan and F. Li, *ChemCatChem*, 2016, **8**, 3769–3779.
117 G. Ding, C. Li, L. Chen and G. Liao, *Energy Environ. Sci.*, 2024, **17**, 5311–5335.
118 Z. Chen, G. Ding, Z. Wang, Y. Xiao, X. Liu, L. Chen, C. Li, H. Huang and G. Liao, *Adv. Funct. Mater.*, 2025, 2423213.
119 G. Ding, C. Li, Y. Ni, L. Chen, L. Shuai and G. Liao, *EES Catal.*, 2023, **1**, 369–391.
120 C. Li, G. Ding, P. Wang, K. Liu, B. Yang and G. Liao, *Dalton Trans.*, 2025, **54**, 889–897.
121 G. Ding, Z. Wang, J. Zhang, P. Wang, L. Chen and G. Liao, *EcoEnergy*, 2024, **2**, 22–44.
122 Q. Zhang, G. Liao, B. Yang, Y. Zhang, G. Ge, A. Lipovka, J. Liu, R. D. Rodriguez, X. Yang and X. Jia, *Appl. Surf. Sci.*, 2023, **638**, 157989.
123 C. Li, N.-Y. Huang, Y. Yang, Q. Xu and G. Liao, *Coord. Chem. Rev.*, 2025, **524**, 216292.
124 F. Tian, X. Wu, J. Chen, X. Sun, X. Yan and G. Liao, *Dalton Trans.*, 2023, **52**, 11934–11940.
125 G. Liao, C. Li, S.-Y. Liu, B. Fang and H. Yang, *Phys. Rep.*, 2022, **983**, 1–41.
126 K. Liu, M. A. Nawaz and G. Liao, *Carbon Neutralization*, 2025, **4**, e190.
127 K. Liu, Y. Liao, P. Wang, X. Fang, J. Zhu, G. Liao and X. Xu, *Nanoscale*, 2024, **16**, 11096–11108.
128 L. Liao, K. Wang, G. Liao, M. A. Nawaz and K. Liu, *Catal. Sci. Technol.*, 2024, **14**, 6537–6549.
129 K. Liu, L. Liao, L. Li, M. A. Nawaz, G. Liao and X. Xu, *Surf. Interfaces*, 2025, **56**, 105496.
130 K. Liu, L. Liao and G. Liao, *Nanoscale*, 2024, **16**, 21783–21793.
131 G. Liao, C. Li, S.-Y. Liu, B. Fang and H. Yang, *Trends Chem.*, 2022, **4**, 111–127.
132 G. Liao, G. Ding, B. Yang and C. Li, *Precis. Chem.*, 2024, **2**, 49–56.
133 J. Huang, X. Li, X. Wang, X. Fang, H. Wang and X. Xu, *J. CO_2 Util.*, 2019, **33**, 55–63.
134 J. Ren, H. Guo, J. Yang, Z. Qin, J. Lin and Z. Li, *Appl. Surf. Sci.*, 2015, **351**, 504–516.
135 E. Oh, J. Kim, J. Jang, N. Lee, J. Sah, H. Jeong, S. W. Lee, D. Y. Kim, S.-Y. Jeon, B.-J. Kim, J. Yang and J. Kim, *Energy Fuels*, 2024, **38**, 22974–22985.
136 M. Ozturk and I. Dincer, *Int. J. Hydrogen Energy*, 2021, **46**, 31511–31522.
137 M. J. B. Kabeyi and O. A. Olanrewaju, *J. Energy*, 2022, **2022**, 8750221.

